CHARACTERIZING EXCITATORY TRANSMISSION IN MELANIN-CONCENTRATING HORMONE NEURONS

by © Sherri C. Bowes

A thesis submitted to the School of Graduate Studies in partial fulfilment of the requirements for the degree of

Master of Science in Medicine (Neuroscience)

Division of Biomedical Sciences, Faculty of Medicine

Memorial University of Newfoundland

October 2020

St. John's, Newfoundland and Labrador

Abstract

Melanin-concentrating hormone (MCH) neurons of the lateral hypothalamus are involved in homeostatic mechanisms including energy balance and sleep wake cycles. Glutamate is an excitatory transmitter that is released by neurons and astrocytes, providing an excitatory control over neuronal activity. Here, I investigated the role of glutamate transporters and glutamate receptors in excitatory signaling onto MCH neurons. Using patch clamp electrophysiology, I have identified three distinct excitatory glutamatergic currents in MCH neurons: fast EPSC, slow EPSC, and tonic currents. I demonstrate that presynaptic train stimulation induces EPSCs with two distinct time courses (fast and slow) while tonic currents are due to ambient glutamate that accumulates when glutamate transporters are inhibited. Furthermore, these currents are mediated by distinct glutamate receptor pools, which are under the regulation of different glutamate transporters. This work contributes to the ongoing understanding of basic excitatory signaling in MCH neurons. Given the known role of MCH in promoting sleep and weight gain this may have functional implications for sleep and energy homeostasis.

Acknowledgments

First and foremost, I want to thank my supervisor, Dr. Michiru Hirasawa and my committee members, Dr. Matthew Parsons and Dr. Xihua Chen. Thank you to all past and present members of the Hirasawa lab family. Special thanks to Lisa Fang, Todd Rowe, Maria Licursi and Nick Newhook for their support with my research and contributions to this thesis. I would also like to thank Dr. Chantalle Briggs and Dr. Kazue Semba for collaborating with me throughout my MSc. Lastly, thank you to my friends and family who have been there since the beginning, supporting me and cheering me on.

Dedicated to my father, David Bowes. I love you, Dad.

Table of Contents

List of Tables

List of Figures

List of Abbreviations

ACSF: Artificial Cerebrospinal Fluid

AMPAR: *a*-amino-3-hydroxy-5-methyl-4-isoxazolepropionic receptor

ANOVA: Analysis of Variance

ATP: Adenosine Triphosphate

C°: Celsius

CNS: Central Nervous System

D-AP5: 2R-amino-5-phosphonovaleric acid

DHK: Dihydrokainic Acid

EAAT: Excitatory Amino Acid Transporter

EPSC: Excitatory Postsynaptic Current

GAD: Glutamic Acid Decarboxylase

GABA: γ-aminobutyric acid

Gi/o: Gi/o protein alpha subunit

GLAST: Glutamate Aspartate Transporter

GLT-1: Glutamate Transporter 1

Gq: Gq protein alpha subunit

GYKI52466: 4-(8-methyl-9*H*-[1,3]dioxolo[4,5-h][2,3]benzodiazepin-5-yl)aniline

h: hour

Hz: Hertz

ICV: Intracerebroventricular

IHC: Immunohistochemistry

IgG: Immunoglobulin G

iGluR: Ionotropic Glutamate Receptor

KAR: Kainate Receptor

kHz: Kilohertz

LH: Lateral Hypothalamus

LY367385: *S*-(+)-α-Amino-4-carboxy-2-methylbenzeneaceticacid

MCH: Melanin-concentrating Hormone

MCHR1: Melanin-concentrating Hormone Receptor 1

MCHR2: Melanin-concentrating Hormone Receptor 2

mGluR: Metabotropic Glutamate Receptor

mL/min: Milliliter per minute

MPEP: 2-methyl-6-phenylethynylpyridine

mM: Millimolar

mmol/kg: Millimolar per kilogram

mRNA: Messenger Ribonucleic Acid

ms: Millisecond

mV: Millivolt

MΩ: Milli Ohm

n: sample size

nM: Nanomolar

NMDAR: N-Methyl-D Aspartate Receptor

ORX: Orexin

pA: picoampere

PSD: Post-Synaptic Density

REM: Rapid Eye Movement

s: second

SEM: Standard Error of the Mean

SLC1: Solute Carrier 1

TFB-TBOA: (2S,3S)-3-(3-[4-(Trifluoromethyl)benzoylamino]benzyloxy)aspartate

TTX: Tetrodotoxin

µm: Micrometer

µM: Micromolar

UBP310: *S*-1-(2-Amino-2-carboxyethyl)-3-(2-carboxy-thiophene-3-yl-methyl)-5-methylpyrimidine-2,4-dione

UCPH101: 2-Amino-5,6,7,8-tetrahydro-4-(4-methoxyphenyl)-7-(naphthalen-1-yl)-5-oxo-4*H*-chromene-3-carbonitrile

VGLUT1: Vesicular Glutamate Transporter 1

1-0 Introduction

1-1 General overview

As the predominant excitatory neurotransmitter in the central nervous system (CNS), glutamate is involved in a variety of physiological brain functions. Glutamate transporters maintain extracellular glutamate concentrations and are critical for optimal signaling and the regulation of receptor activation. Glutamate acts on a variety of ionotropic and metabotropic receptors that can be expressed in unique subcellular domains, synaptically or extrasynaptically, adding an extra layer to the complexity of glutamatergic transmission. How glutamate signaling is regulated varies from synapse to synapse. In this thesis I will investigate glutamatergic signaling in melanin-concentrating hormone (MCH) neurons of the hypothalamus, a cell population known to regulate homeostatic mechanisms. With the goal to eventually understand how excitatory transmission is implicated in homeostatic regulation and dysregulation we must first characterize glutamatergic signaling in the normal condition.

1-2 Glutamate is the major excitatory neurotransmitter in the brain

Glutamate is an excitatory neurotransmitter that contributes to most aspects of normal brain function including learning and memory, cognition, and development of the central nervous system (Danbolt, 2001). Abnormal brain function or pathogenesis of neurological disorders can often be attributed to glutamate (Danbolt, 2001; Vandenberg and Ryan, 2013). Excessive glutamate can be toxic to neurons and lead to cell death, therefore it is crucial that glutamate concentrations are kept low (Danbolt, 2001; Zhou and Danbolt,

2014). Overall, concentrations of glutamate are higher than any other amino acid in the brain (5-15 mmol/kg brain tissue), making it the most abundant excitatory neurotransmitter in the mammalian central nervous system (Schousboe, 1981). The majority of this glutamate is located intracellularly with the highest concentrations at nerve terminals (Ottersen et al., 1992). Extracellular concentrations in the interstitial space make up only a small fraction of total brain glutamate and have been estimated to range from 25-90 nM in acute brain slices while *in vivo* microdialysis estimates range from 0.2-35 μM (Herman and Jahr, 2007; Chiu and Jahr, 2017).

1-3 General overview of excitatory neurotransmission

Typical excitatory transmission involves release of glutamate from the presynaptic neuron, diffusion of glutamate within the synaptic cleft, binding of postsynaptic glutamate receptors and subsequent intracellular signaling, and clearance of synaptic glutamate resulting in termination of postsynaptic excitation. The process begins with the synthesis and packaging of glutamate into synaptic vesicles within the presynaptic nerve terminal (Hackett and Ueda, 2015). Arrival of an action potential at the presynaptic terminal leads to calcium influx as voltage gated calcium channels open (Rusakov, 2009). This calcium transient triggers exocytosis, namely fusion of synaptic vesicles with the plasma membrane, and release of neurotransmitter into the synaptic cleft (Augustine, 2001). It is important to note that while calcium influx is required for action potential evoked release it is typically not needed for spontaneous release of glutamate (Vyleta and Smith, 2011; Hackett and Ueda, 2015). In addition, non-vesicular (i.e. non-exocytotic)

mechanisms of glutamate release have been shown during blockade of voltage gated calcium channels and voltage gated sodium channels by cadmium and tetrodotoxin, respectively (Danbolt, 2001).

Once released, glutamate immediately diffuses into the synaptic cleft. The time course of this diffusion is determined by the anatomy and complexity of the synapse (Danbolt, 2001). Glutamate first binds with synaptic receptors directly opposing the site of release clustered within the post synaptic density (PSD). As glutamate continues to diffuse away from the site of release, it can reach the synaptic perimeter and bind receptors in the perisynaptic zone (the 100-200 nm ring surrounding the PSD) (Scheefhals and MacGillavry, 2018). Further diffusion may allow glutamate to activate extrasynaptic receptors (those beyond the 100-200 nm perisynaptic ring) and ultimately contact glutamate transporters which terminate neurotransmission by removing glutamate from the extracellular space (Danbolt, 2001; Scheefhals and MacGillavry, 2018). It is difficult to determine exact morphological boundaries for these zones and it is likely that there is some degree of overlap, depending on the type of synapse. Generally, it is accepted that synaptic receptors are activated by low frequency afferent activity and spontaneously released glutamate, while perisynaptic and extrasynaptic receptors are activated by synaptic spillover during higher frequency afferent activity (Papouin and Oliet, 2014; Scheefhals and MacGillavry, 2018).

1-4 Ionotropic and metabotropic glutamate receptors

There are two functionally distinct families of glutamate receptors: ionotropic and metabotropic. Ionotropic glutamate receptors (iGluRs) are ligand gated ion channels which open upon direct binding of the ligand to allow the passage of specific ions. These receptors are typically expressed postsynaptically and produce excitatory currents (Reiner and Levitz, 2018). iGluRs respond on the millisecond timescale and mediate the majority of fast synaptic transmission (Scheefhals and MacGillavry, 2018). The three main subfamilies of iGluRs are AMPA receptors (AMPARs), NMDA receptors (NMDARs) and kainate receptors (KARs) (Hollmann, 1994). Assembled as tetramers, iGluRs have an extracellular N-terminus, an intracellular C-terminus, an extracellular ligand binding domain , and a pore forming transmembrane domain which forms a cation permeable channel (Traynelis, 2010; Reiner and Levitz, 2018).

Metabotropic receptors (mGluRs) are G protein coupled receptors that undergo a conformational change upon ligand binding, activating intracellular signaling cascades through second messengers (Niswender and Conn, 2010). mGluRs are slower to respond compared to iGluRs but their effects are longer lasting (Scheefhals and MacGillavry, 2018). mGluRs are subdivided into three groups: group I are primarily G_q coupled and located postsynaptically while group II and III are $G_{i/o}$ coupled and involved in presynaptic inhibition (Reiner and Levitz, 2018).

In addition to the spatial organization of individual receptors, different affinities for glutamate determine the likelihood of that receptor being activated. In addition to binding

affinity, the number of glutamate molecules that bind impacts the probability of the channel opening (Scheefhals and MacGillavry, 2018). AMPARs are relatively low affinity, NMDARs are higher affinity and KARs can be high or low affinity depending on the tetramer subunit composition (Hollmann, 1994; Danbolt, 2001; Fisher and Mott, 2011; Scheefhals and MacGillavry, 2018). mGluRs exhibit a low affinity for glutamate, similar to AMPARs (Scheefhals and MacGillavry, 2018).

1-5 Termination of glutamatergic transmission

For dynamic signaling processes with a high signal-to-noise ratio, it is crucial that extracellular glutamate concentrations are kept low. There are no enzymes present extracellularly to degrade glutamate, therefore, glutamate must be physically removed via cellular uptake (Danbolt, 2001). Glutamate transporters are responsible for clearing glutamate from the extracellular space, controlling synaptic spillover and preventing overexcitation of receptors (Danbolt, 1994; Vandenberg and Ryan, 2013).

Glutamate transporters are divided into five subtypes of Excitatory Amino Acid Transporters (EAAT1-5) which are expressed in different brain regions and cell types (Lehre and Danbolt, 1998). GLT-1 (EAAT2) is considered the most abundant glutamate transporter as it makes up 1% of total forebrain protein and has been suggested to account for up to 90% of total glutamate uptake in the brain (Lehre and Danbolt, 1998; Grewer et al., 2014). GLT-1 is predominantly expressed on astrocytes but can be expressed in synaptic terminals of neurons (Furness et al., 2008; Grewer et al., 2014). GLAST (EAAT1) is an astrocytic glutamate transporter that is often co-expressed alongside GLT-

1 in astrocytic membranes (Haugeto et al., 1996). Overall, the density of GLAST is less than that of GLT-1, except in the cerebellum where GLAST is 6-fold more abundant than GLT-1 (Lehre and Danbolt, 1998). EAAC1 (EAAT3) is a neuronal transporter that is expressed in somata and dendrites and not found in axon terminals (Holmseth et al., 2012). In the rat hippocampus, expression of EAAC1 is approximately 100-fold less than GLT-1 and GLAST and only 30% of EAAC1 is localized to the plasma membrane (Holmseth et al., 2012). While EAAC1 immunoreactivity is distributed throughout dendrites and somata, the low expression level of this protein raises a question about its role in glutamate clearance when compared to the abundantly expressed GLT-1 (Holmseth et al., 2012). Scimemi et al. (2009) found that EAAC1 regulates the time course of glutamate in the extracellular space by rapidly binding and unbinding the transmitter. In this way, rather than rapidly uptaking glutamate itself, EAAC1 can serve to buffer extracellular glutamate concentrations, prolonging the glutamate transient and the time for astrocytic transporters to transport glutamate. It was also found that EAAC1 reduced NMDAR activation, suggesting that buffered glutamate slowly unbinds from EAAC1 which is likely to be immediately cleared by glial transporters. These findings indicate that functionally, EAAC1 may be more involved in modulating the accessibility of glutamate to other transporters instead of directly regulating neurotransmission (Scimemi et al., 2009). EAAT4 is a neuronal transporter with greatest expression in the Purkinje cells of the cerebellum (Dehnes et al., 1998). EAAT5 is found exclusively in the retina with expression in both rod and cone terminals (Arriza et al., 1997).

1-6 Mechanisms of glutamate transport

The five EAAT subtypes discussed here are members of the solute carrier 1 (SLC1) family. These transmembrane proteins are secondary active transporters that uptake glutamate against its concentration gradient, which is several thousand fold across the plasma membrane (Danbolt, 2001; Grewer et al., 2014). The driving force for transport of one individual glutamate molecule is cotransport of 3 Na+ ions and 1 proton into the cell and counter transport of 1 K+ ion out of the cell (Zerangue and Kavanaugh, 1996). The ability of transporters to uptake glutamate is described by the alternating access model which states that transporters undergo a conformational change exposing the extracellular ligand binding domain to the intracellular surface where the ligand is released (Oleg, 1966). The kinetics of transport depend on the binding rate of glutamate, the likelihood that the ligand will be released intracellularly, the density of transporters near the synapse and the turnover rate of the transporter which is the time needed to complete one full transport cycle (Vandenberg and Ryan, 2013).

1-7 Gliotransmission

Outnumbering neurons 10:1, glial cells are now widely accepted as active participants in neurotransmission (Kurosinski et al., 2002). One individual astrocyte can contact thousands of synapses suggesting that astrocytes partner with neurons to modulate neural communication (Tasker et al., 2012). Astrocytes play a crucial role in glutamate homeostasis as they express high affinity glutamate transporters responsible for glutamate reuptake (Danbolt, 2001; Tasker et al., 2012). In this way, astrocytes regulate extracellular concentrations of glutamate, limiting receptor activation and diffusion to

nearby synapses (Tasker et al., 2012). Furthermore, astrocytes are known to release gliotransmitters such as glutamate, GABA, ATP, and adenosine into the extracellular space (Tasker et al., 2012). Although incapable of producing action potentials, astrocytes can release gliotransmitters in a calcium dependent manner, similarly to neurons. Termed "calcium excitability", astrocytes can produce calcium waves by changing their intracellular calcium concentration (Pál, 2015). In addition to calcium dependent exocytosis, astrocytes can release gliotransmitters through hemichannels, anion channels, purinergic receptors and reverse mode transporters (Pál, 2015). Clearly, astrocytes are not solely structural support for neurons but important contributors to complex functions of the CNS.

1-8 Synaptic vs ambient glutamate

There are two distinct ways to categorize extracellular glutamate: synaptic and ambient. Synaptic glutamate is confined to the synaptic cleft and its levels are directly influenced by both spontaneous and action-potential-dependent release from the presynaptic terminal. Approximately 4000 molecules of glutamate are contained within a single synaptic vesicle which are released during excitatory transmission, causing the concentration of synaptic glutamate to undergo a rapid transient increase (Marx et al., 2015). The concentration of glutamate within the synapse depends on how much glutamate was released, the size of the synapse, how many transporters are available for reuptake and where these transporters are located (Danbolt, 2001). Transporters expressed within the vicinity of the synapse, especially those near release sites, have a direct ability to control synaptic concentrations and regulate receptor activation. Transporters

expressed at the synaptic perimeter are more likely to prevent spillover into the extrasynaptic space and prevent or allow diffusion back into the synaptic cleft (Danbolt, 2001).

Ambient glutamate refers to the low concentration of non-synaptic glutamate that is always present in the extracellular space (Tasker et al., 2012). While conventional vesicular release from neurons can contribute to ambient glutamate levels by synaptic spillover and diffusion from nearby synapses, ambient glutamate concentrations are influenced by non-neuronal factors, such as gliotransmission (Cavelier et al., 2005; Le Meur et al., 2007). Since astrocytes possess both glutamate release and glutamate reuptake mechanisms, these cells are recognized as major regulators of ambient glutamate concentrations (Jourdain et al., 2007; Tasker et al., 2012).

1-9 Role of synaptic and extrasynaptic receptors

Synaptic and ambient glutamate act on distinct pools of receptors. Synaptic glutamate binds low-affinity, rapidly desensitizing receptors within the PSD and these responses can be recorded as excitatory postsynaptic currents (EPSCs) (Tasker et al., 2012). EPSCs are fast, phasic responses which last in the order of milliseconds. Conversely, ambient glutamate has been shown to bind extrasynaptic receptors with greater affinity and less desensitization (Tasker et al., 2012). This activity induces tonic currents which are distinguishable from EPSCs as they are persistent, lasting several minutes (Tasker et al., 2012).

Le Meur et al (2007) found that ambient glutamate of glial origin activates extrasynaptic NMDARs in a tonic manner in the hippocampus. Tonic activation of NMDARs by ambient glutamate was also observed in pyramidal cells and interneurons of the prefrontal cortex (Povysheva and Johnson, 2012). NMDAR-mediated tonic current has been found to be upregulated in pathological conditions such as Alzheimer Disease (Papouin and Oliet, 2014). Tonic activation of extrasynaptic receptors has also been shown to be involved in development and reward, and may have neuroprotective effects (Cavelier et al., 2005; Povysheva and Johnson, 2012)

Extrasynaptic receptors were once considered a non-functional reserve pool, however, it is now recognized that their signaling plays an important role in information processing (Harney et al., 2008). Synaptic- and extrasynaptic-mediated signaling may also result in functionally distinct outcomes. Hardingham et al (2002) showed that synaptic NMDAR activation led to anti-apoptotic activity while extrasynaptic NMDAR activation resulted in cell death of hippocampal neurons. These differences support the notion of compartmentalized signaling mechanisms induced by synaptic and ambient glutamate. Therefore, understanding the source of ambient glutamate and where it acts is of utmost importance to expanding our knowledge of glutamatergic signaling. Moreover, this highlights the importance of studying different receptor pools in distinct subcellular domains.

1-10 The lateral hypothalamus

The lateral hypothalamus (LH) is one of the most well-connected areas of the brain, containing an intricate assembly of complex neural connections. It receives inputs from many brain areas and integrates this information to coordinate homeostatic mechanisms (Bonnavion et al., 2016). Neurons of the LH have widespread projections throughout the CNS including the forebrain and brainstem (Bittencourt et al., 1992; Meister, 2007; Barbosa et al., 2017). The LH is an extremely heterogenous region containing diverse nuclei and cell types which work together to regulate feeding behavior, energy balance and sleep-wake states (Meister, 2007; Hahn and Swanson, 2010; Brown et al., 2015). Sleep-wake balance is primarily regulated by alternate activation of the sleep and wake promoting neurons in the LH: orexin (ORX) and melanin concentrating hormone (MCH) (Bonnavion et al., 2016; Briggs et al., 2018). Orexin neurons promote wakefulness while MCH neurons promote sleep. Furthermore, both cell populations stimulate feeding behaviour and play an integral part in energy balance (Meister, 2007).

Glutamate is the dominant excitatory neurotransmitter in hypothalamic control of homeostasis (Meister, 2007). For example, when glutamate is injected into the LH it elicits an immediate feeding response, perhaps through its actions on orexigenic neural populations (Meister, 2007). Glutamate transporters GLT-1, GLAST and EAAC1 are expressed in the hypothalamus and are likely to play significant roles in homeostatic functions. However, their role in regulating LH neurons is poorly understood.

1-11 Melanin-concentrating hormone (MCH) neurons

Melanin concentrating hormone is a 19 amino acid cyclic neuropeptide that is synthesized exclusively by neurons of the LH and zona incerta (Bittencourt et al., 1992). The peptide was originally discovered in teleost fish as a skin pigmentation modulator but MCH was later found in the brains of humans and rats (Kawauchi et al., 1983; Bittencourt et al., 1992). MCH is a ligand for the receptors MCHR1 and MCHR2. In humans, both receptors types are expressed throughout the brain, however, rodents only express MCHR1 (Chee et al., 2014). MCHR1 is a $G_{i/o}$ coupled receptor and MCHR2 is G_q coupled, suggesting that MCH can exert either inhibitory or excitatory effects (Chee et al., 2014). MCH neurons are also capable of releasing classical neurotransmitters glutamate and GABA as they have been found to express VGLUT1 and GAD65/67 (Harthoorn et al., 2005; Meister, 2007).

MCH neurons are known to promote feeding behaviour and are also involved in REM sleep. Overexpression of MCH in mice leads to hyperphagia and increased body weight while mice with an MCH deletion are hypophagic and lean (Shimada et al., 1998; Ludwig et al., 2001). Intracerebroventricular (ICV) injection of MCH stimulates food intake and during fasting mRNA levels of MCH are increased (Meister, 2007). MCH neurons are active during REM sleep and injections of MCH into the dorsal raphe nucleus induce dose dependent increases in REM sleep (Verret et al., 2003; Lagos et al., 2009). Further, MCH neurons project to the brainstem which has known roles in the regulation of sleep wake states (Ludwig et al., 2001). In summary, MCH neurons play critical roles in wide-ranging physiological functions. Thus, it is important to understand the cellular

mechanisms that influence the excitability of these neurons, which may have implications for regulation and dysregulation of homeostasis.

1-12 Rationale and Hypotheses

As glutamate is the major excitatory neurotransmitter in the hypothalamus, activity of MCH neurons is regulated by glutamate. Therefore, the goal of this project is to better understand the basic mechanisms of glutamatergic transmission in MCH neurons. As MCH is known to promote weight gain and sleep, these findings may have implications in homeostatic mechanisms such as energy balance and sleep-wake behaviour. Interestingly, previous work in our lab describes how MCH neurons display unique biphasic EPSCs consisting of a fast phase immediately following each synaptic stimulation and a slow phase which persists after synaptic stimulation has ended (Briggs et al., 2018). Our lab has also found that homeostatic challenge impacts excitatory transmission to MCH neurons. When rats were sleep deprived for 6h, there was a selective decrease in slow EPSC, but not fast EPSC, compared to control rats who were permitted to rest. This decrease was accompanied by increased apposition of GLT-1 to MCH soma, which indicates that greater glutamate clearance is responsible for the decrease in slow EPSCs (Briggs et al., 2018). This finding suggests an important role for glutamate transporters in the regulation of excitatory synaptic transmission in MCH neurons under normal conditions and homeostatic challenge in the form of sleep deprivation. Furthermore, it indicates that distinct mechanisms exist for fast and slow EPSCs. However, it remains to be explored whether glutamate transporters regulate tonic currents in these neurons. These findings lead to the following hypotheses

Hypotheses

In MCH neurons,

1. EPSCs and tonic currents are mediated by different glutamate receptor pools.
2. EPSCs and tonic currents are differentially regulated by glutamate transporters.

2-0 Methods

2-1 Animals

All procedures were conducted in accordance with the Canadian Council on Animal Care and were approved by the Memorial University Institutional Animal Care Committee. Male Sprague Dawley rats were obtained from Charles River Canada (St. Constant, QC, Canada). Animals were single housed under a 12h light/12h dark cycle (lights on at 08:00) in the animal care facility in the Faculty of Medicine. Animals were fed standard rodent chow (Teklad 2018 rodent diet, Envigo). Animals had access to food and water ad libitum. Experiments were performed on brain slices from rats aged between 7 and 10 weeks.

2-2 In Vitro Electrophysiology

Rats were deeply anesthetized with isoflurane, decapitated and brains quickly removed. Coronal slices (250 µm thick) of the hypothalamus were cut in ice cold artificial cerebrospinal fluid (ACSF) containing (in mM): 126 NaCl, 2.5 KCl, 1.2 NaH_2PO_4, 1.2 $MgCl_2$, 18 $NaHCO_3$, 2.5 glucose, 2 $CaCl_2$. Slices were then incubated in ACSF at 32-34 °C for 30 minutes and then left at room temperature until recording. ACSF was continuously bubbled with O_2 (95%) and CO_2 (5%).

Patch clamp recordings were performed on hemisected hypothalamic slices superfused with 27-30 C° ACSF at 2.5-3.0mL/min. Neurons that were located in the lateral hypothalamic area and zona incerta (dorsomedial to the fornix, midway to the

mammillothalamic tract) and had a large soma diameter (10-20 µm) were selected for recording using a differential interference contrast microscope (DM LFSA; Leica Microsystems). Recordings were performed using a Multiclamp 700B amplifier and pClamp 10.3 software (Molecular Devices, Sunnyvale, CA). The whole-cell internal solution contained (in mM): 123 potassium gluconate, 2 $MgCl_2$, 8 KCl, 10 Hepes, 0.2 EGTA, 5 Na_2-ATP, 0.3 Na-GTP, adjusted to pH 7.29-7.30 with KOH. Biocytin (0.1-0.2%; Sigma Aldrich Canada, Oakville, ON, Canada) was added to the internal solution to label recorded cells. Filled recording electrodes had a tip resistance of 3-7MΩ. Picrotoxin (50 µM; Sigma Aldrich Canada, Oakville, ON, Canada) was always present in the bath during recordings to block $GABA_A$ receptors and isolate excitatory currents.

Once whole cell access was achieved, we characterized the cell type based on its electrophysiological properties using a series of hyperpolarizing and depolarizing current steps (600 ms each ranging from -200 pA to +200 pA). MCH neurons were first identified by their well-established electrophysiological properties (Fig. 1A). MCH neurons are not spontaneously active *in vitro*, have a hyperpolarized resting membrane potential, lack H-current and rebound depolarization, and display spike adaptation upon positive current injection (Alberto et al., 2011). Following recording, experimental brain slices were fixed in 10% formalin and processed for post hoc immunohistochemistry to confirm the neurochemical identity of recorded biocytin-filled cells (below).

For EPSC recording, neurons were held at -70 mV and membrane currents were filtered at 1 kHz, digitized at 10 kHz and stored for offline analysis. To record evoked EPSCs, a

glass stimulating electrode was placed approximately 100 µm away from the recorded cell in order to stimulate afferent fibers. Train stimulation consisting of 20 pulses at 50 Hz was applied every 30 seconds. Once evoked responses were stable (the first EPSC at least 150 pA), a baseline was recorded for 5 minutes. Following the baseline, various drugs were bath applied for 5 minutes each and then were washed in normal ACSF for a minimum of 10 minutes. In some cases, multiple drugs were co-applied or applied in sequence for up to 15 minutes prior to washing. The peak amplitude of the fast EPSCs following the first and second pulses were measured. Slow EPSC amplitude was measured 25 ms after the final stimulation artifact, as our pilot study indicated that the fast EPSC completely decayed within 25 ms. The slow EPSC area was defined as the area under the curve between 25 and 750 ms after the final stimulation artifact. A 20 mV hyperpolarizing pulse (100 ms) was applied every 30 s, and the steady state and capacitive currents were monitored as measures of input and access resistance, respectively. Cells that showed significant change (>20%) in these parameters during electrophysiological recordings were excluded from analysis.

For tonic currents, all recording procedures were identical to those described above, except without synaptic stimulation. The peak amplitude of the tonic current was identified and measured.

2-3 Post Hoc Immunohistochemistry

After recording, brain slices were immediately placed in 10% formalin and fixed for >24h at 4C°. To confirm the phenotypes of recorded cells, fixed slices were individually

incubated with rabbit anti-MCH IgG (1:2000; G-070-47; Phoenix Pharmaceuticals) for 3 days at 4C°. Next, slices were incubated overnight at 4°C with Alexa 594-conjugated donkey anti-rabbit IgG (1:500; A21207; Invitrogen) as well as Alexa 350-conjugated streptavidin (1:500; Jackson ImmunoResearch, West Grove, PA, USA) to visualize MCH peptide and biocytin in recorded cells, respectively. Stained slices were examined with an epifluorescence microscope to determine co-localization of MCH with biocytin. A total of 129 cells from 74 rats showed electrophysiological properties typical of MCH neurons and were included in the analysis for this study. Among these 129 cells, fluorescent biocytin labelling was present in 95 cells and MCH immunolabelling was confirmed in 100% of these biocytin filled neurons (95 of 95). An example of an MCH neuron co-labelled with biocytin and proMCH (precursor of MCH peptide) is shown in figure 1B.

2-4 Drugs

All drugs were aliquoted and frozen as 1000x stock solutions. Immediately before use, aliquots were thawed, diluted into ACSF and bath applied. Tetrodotoxin (TTX) was purchased from Alomone Labs (Jerusalem, Israel). GYKI52466 was purchased from Hello Bio (Bristol, UK). DAP5 and UBP310 were purchased from Abcam (Toronto, ON, Canada). TFB-TBOA, UCPH101, DHK, MPEP, and LY367385 were purchased from Tocris Bioscience (Minneapolis, MN, USA). See Table 1 for complete list of bath applied drugs.

2-5 Data Analysis

EPSCs and tonic currents were analyzed using Clampfit 10.7 software (Molecular Devices, Sunnyvale, CA). Statistical analyses were conducted with Prism 8 (GraphPad Software, La Jolla, CA). To compare the drug effect to its baseline, paired t tests were used. To compare different drug effects between cells, unpaired t tests were used. For group comparisons of different drugs or different concentrations of the same drug, one-way ANOVA was used. Tukey's or Dunnet's post-hoc analysis was used for multiple comparisons as appropriate. P values <0.05 were considered statistically significant. Values are expressed as means+/- SEM. N-values indicate both the number of animals used and the number of cells included in each experiment. In cases where the same set of cells is analyzed more than once, the n-values are mentioned only on the first occasion.

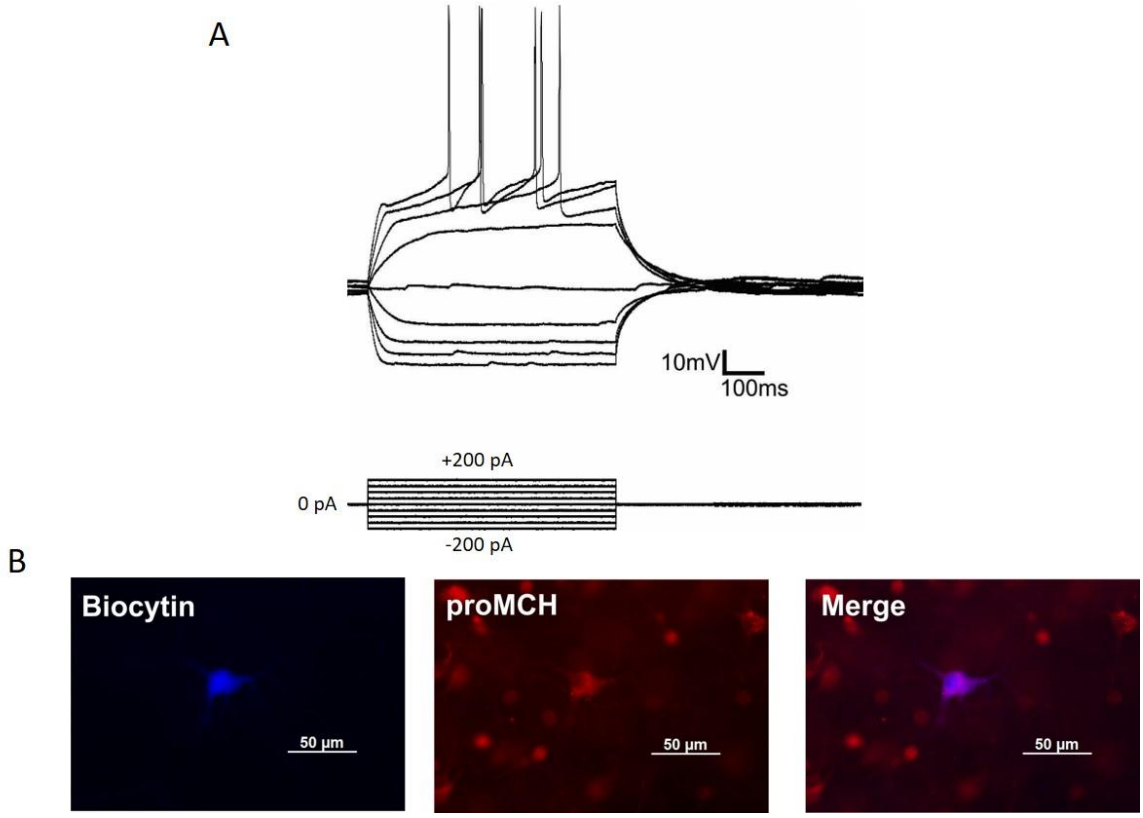

Fig 1. Identification of MCH neurons.

A) Electrophysiological fingerprint of an MCH neuron during a series of positive and negative current injections. These cells typically lack H-current and spontaneous firing while exhibiting spike adaptation.
B) Patched cells were filled with biocytin for post-hoc immunohistochemistry. Images show a cell colabelled with biocytin and proMCH.

Drug	Function	Conc.	Catalog #	Source
TTX	Na+ channel blocker	1 µM	T-500	Alomone Labs
Picrotoxin	$GABA_A$ channel blocker	50 µM	P1675	Sigma Aldrich Canada
GYKI52466	AMPAR antagonist	100 µM	HB0311	Hello Bio
DAP5	NMDAR antagonist	50 µM	Ab120003	Abcam
UBP310	KAR antagonist	10 µM	Ab120168	Abcam
MPEP	mGluR5 antagonist	20 µM	1212	Tocris Bioscience
LY367385	mGluR1 antagonist	100 µM	1237	Tocris Bioscience
TFB-TBOA	Non-specific glutamate transporter inhibitor	5 µM	2532	Tocris Bioscience
DHK	GLT-1 inhibitor	100 µM	0111	Tocris Bioscience
UCPH101	GLAST inhibitor	50-100 µM	3490	Tocris Bioscience

Table 1. Drugs added to ACSF for bath application.

3-0 Results

3-1 MCH neurons display biphasic EPSC

To investigate the characteristics of excitatory transmission in MCH neurons, EPSCs were elicited using 50Hz, 20 pulse train stimulation applied to the afferent fibers. This stimulation protocol revealed biphasic EPSCs, consisting of a "fast" and a "slow" component. Typical fast EPSCs are observed immediately following each pulse (Fig 2; red), while the more subtle, slow component accumulates with repeated stimuli and persists after the train stimulation has ended (Fig 2; yellow) as previously described by our laboratory (Briggs 2018). While these phases exhibit some overlap in timing (Fig 2; orange gradient), they can be analyzed individually. Specifically, the peak of first EPSC largely consists of the fast component, whereas the recovery following the train stimulation can represent the slow component.

3-2 Fast and slow EPSCs are mediated by distinct glutamate receptor types

AMPA receptors are well established as the primary mediator of fast EPSCs in the brain, in large part due to their rapid kinetics (Jonas, 2000). Conversely, slow EPSCs have been shown to be mediated by KARs (Castillo, 1997), AMPARs (Lu 2017) and mGluRs (Huang 2007). NMDARs can also mediate slow EPSC (Steinert et al., 2010), although their contribution is unlikely because Mg^2 ions should block NMDA channels in our recording condition in which the cells are recorded at the holding potential of -70 mV. Since synaptically released glutamate may spill over during train stimulation and activate different subset of receptors, biphasic EPSCs in MCH neurons may be mediated by

different glutamate receptor types. Specifically, we hypothesized that the fast EPSCs would have a greater contribution from synaptic iGluRs and that the slow EPSC would have greater contribution from extrasynaptic mGluRs. To determine which glutamate receptors were involved in fast and slow EPSCs, we tested specific iGluR and mGluR antagonists. Indeed, visual inspection of EPSCs during baseline and during specific glutamate receptor antagonists (Fig 3, left) and subtracted traces (i.e. the difference between baseline and antagonist) indicates the distinct contribution of each receptor type to fast and slow EPSC (Fig 3, right). The larger the subtracted trace, the greater the contribution from that receptor type.

Fast EPSCs were found to be primarily AMPAR mediated, as the AMPAR-specific antagonist GYKI52466 (100 µM) decreased the first fast EPSC amplitude by almost 50% (paired t test, $t(5) = 6.08$; $p = 0.0017$; n = 6 cells; n = 5 rats; Fig 4A1,C). The KAR antagonist UBP310 (10µM) decreased fast EPSC amplitude by approximately 20% (paired t test, $t(6) = 4.35$; $p = 0.0043$; n = 7 cells; n = 5 rats; Fig 4A2,C) and the mGluR1 antagonist LY367385 (100 µM) led to a 25% decrease (paired t test, $t(6) = 5.35$; $p = 0.0017$; n = 7 cells; n = 3 animals; Fig 4A5,C) indicating a role of KAR and mGluR1 in fast EPSC. The paired pulse ratio (PPR; a ratio of the amplitude of EPSC2/EPSC1) was found to be significantly increased in the presence of the mGluR1 antagonist LY367385 (paired t test, $t(6) = 3.54$; $p = 0.0122$; n = 7 cells; n = 3 rats; Fig 4B5,D) but not by other receptor antagonists. As an increase in PPR is suggestive of a decrease in presynaptic release probability, this result suggests that mGluR1 modulates EPSCs presynaptically.

In the same set of cells, we next analyzed the slow EPSC. The slow EPSC was found to be mediated by a combination of AMPARs, KARs and NMDARs. The amplitude of the slow EPSC decreased in the presence of GYKI52466 (100 µM) (paired t test, $t(5) = 4.87$; $p = 0.0046$; Fig 5A1,D), UBP310 (10 µM) (paired t test, $t(6) = 5.07$; $P = 0.0006$; Fig 4A2,D), and DAP5 (50 µM) (paired t test, $t(6) = 2.80$; $p = 0.0310$; Fig 5A3,D). LY367385 (100 µM) also decreased the slow EPSC amplitude indicating a contribution from mGluR1 (paired t test, $t(6) = 3.26$; $p = 0.0172$; Fig 5A5,D). In a comparable manner, GYKI52466 (paired t test, $t(5) = 3.44$; $p = 0.0184$; Fig 5B1,E), UBP310 (paired t test, $t(6) = 4.83$, $p = 0.0008$; Fig 5B2,E), and DAP5 (paired t test, $t(6) = 2.81$; $p = 0.0306$; Fig 5B3,E) all decreased the slow EPSC area. There was a contribution from mGluR1 as LY367385 decreased the slow EPSC area (paired t test, $t(6) = 2.63$; $p = 0.0387$; Fig 5B5,E). The decay time of the slow EPSC, defined as the time to decay from 90% to 10% of the peak, was unaffected by glutamate receptor antagonists (Fig 5C1-5,F). MPEP (20 µM), the antagonist for mGluR5 had no effect on slow EPSC amplitude, area or decay time (Fig 5A4,B4,C4).

These results suggest that fast and slow EPSCs are mediated by different, but overlapping, glutamate receptor types in MCH neurons. AMPARs, KARs and mGluR1 contribute to fast EPSCs while AMPARs, KARs, NMDARs and mGluR1 contribute to the slow EPSC.

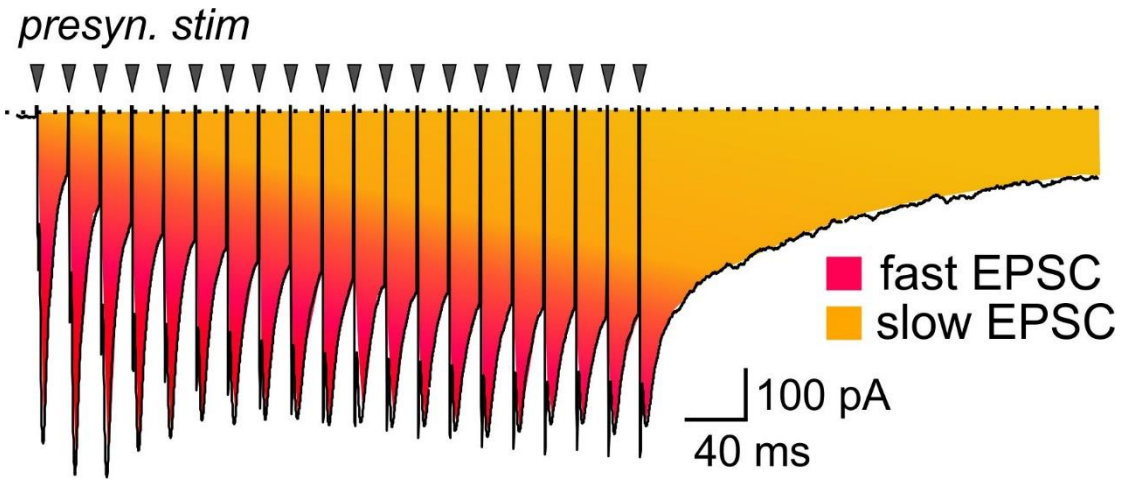

Fig 2. MCH neurons display biphasic excitatory post synaptic currents (EPSC).

Example voltage clamp trace illustrating biphasic EPSC evoked by 50Hz 20 pulse presynaptic train stimulation (presyn. stimulation; arrow heads). Fast EPSCs (red) appear as downward deflections immediately following each stimulation and are fast to peak and decay. Slow EPSC (yellow) develops with repeated stimulation and gradually decays back to baseline after the train has ended. The gradient of colors is used to illustrate the overlap between the fast and slow phases.

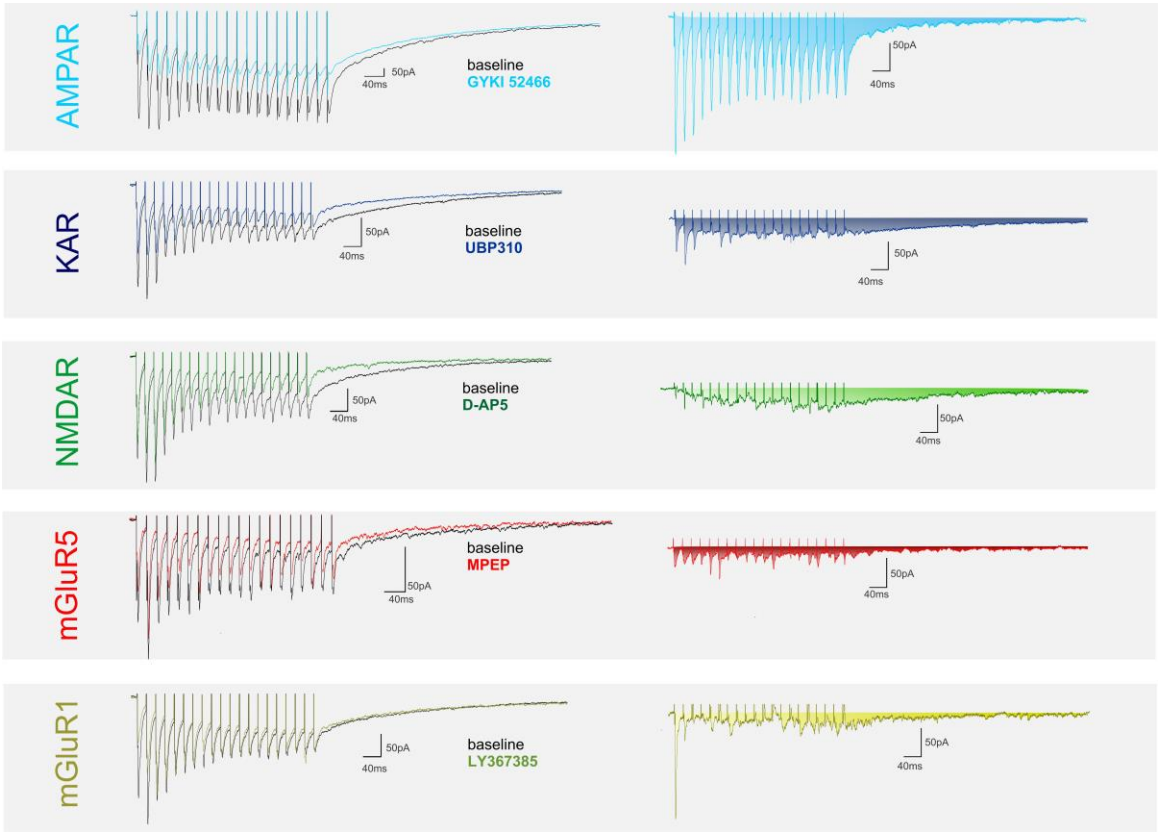

Fig 3. Effect of glutamate receptor antagonists on evoked biphasic EPSCs in MCH neurons.

Left: Superimposed averaged traces of biphasic EPSCs evoked by train stimulation recorded from representative MCH neurons during baseline (black traces) and during glutamate receptor antagonists (colored traces).
Right: subtracted traces illustrating the difference between the baseline and the antagonist traces shown on the left. The subtracted traces represent the current sensitive to each specific receptor antagonist.
To allow visual comparison of superimposed traces (left), the baseline traces of each example are scaled so that their first EPSC is the same size, and the antagonist traces are scaled with their respective baseline traces. Furthermore, the relative scale of the subtracted traces (right) are kept consistent with each other to demonstrate the relative contribution of different receptors.

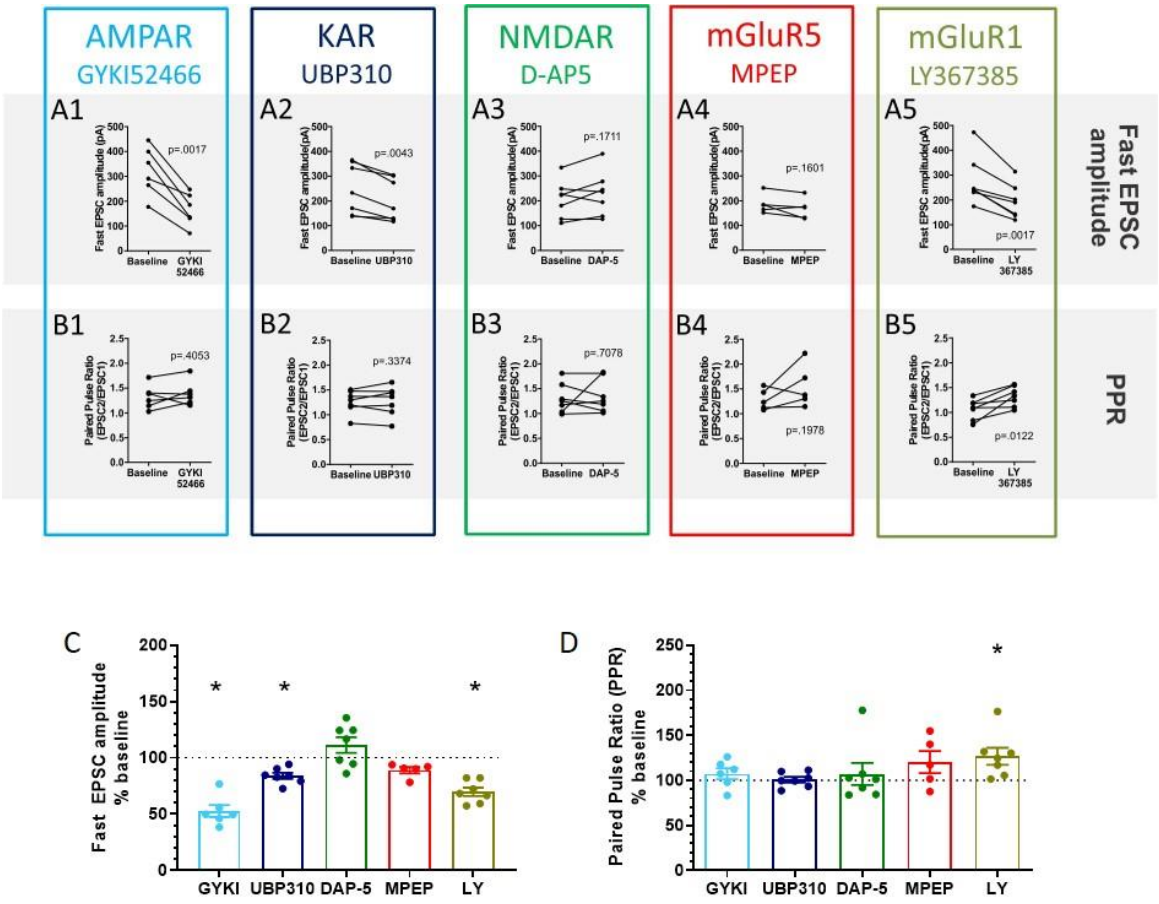

Fig 4. Fast EPSCs are primarily mediated by AMPAR in MCH neurons

Top: Raw values are shown for fast EPSC amplitude **(A1-A5)** and paired pulse ratio (PPR; **B1-B5**). Each connected set of two data points represents one MCH neuron before and during glutamate receptor antagonists.
Bottom: Data is grouped and shown as percent baseline to compare the relative contribution of each glutamate receptor **(C-D).** *p<0.05 vs. baseline.

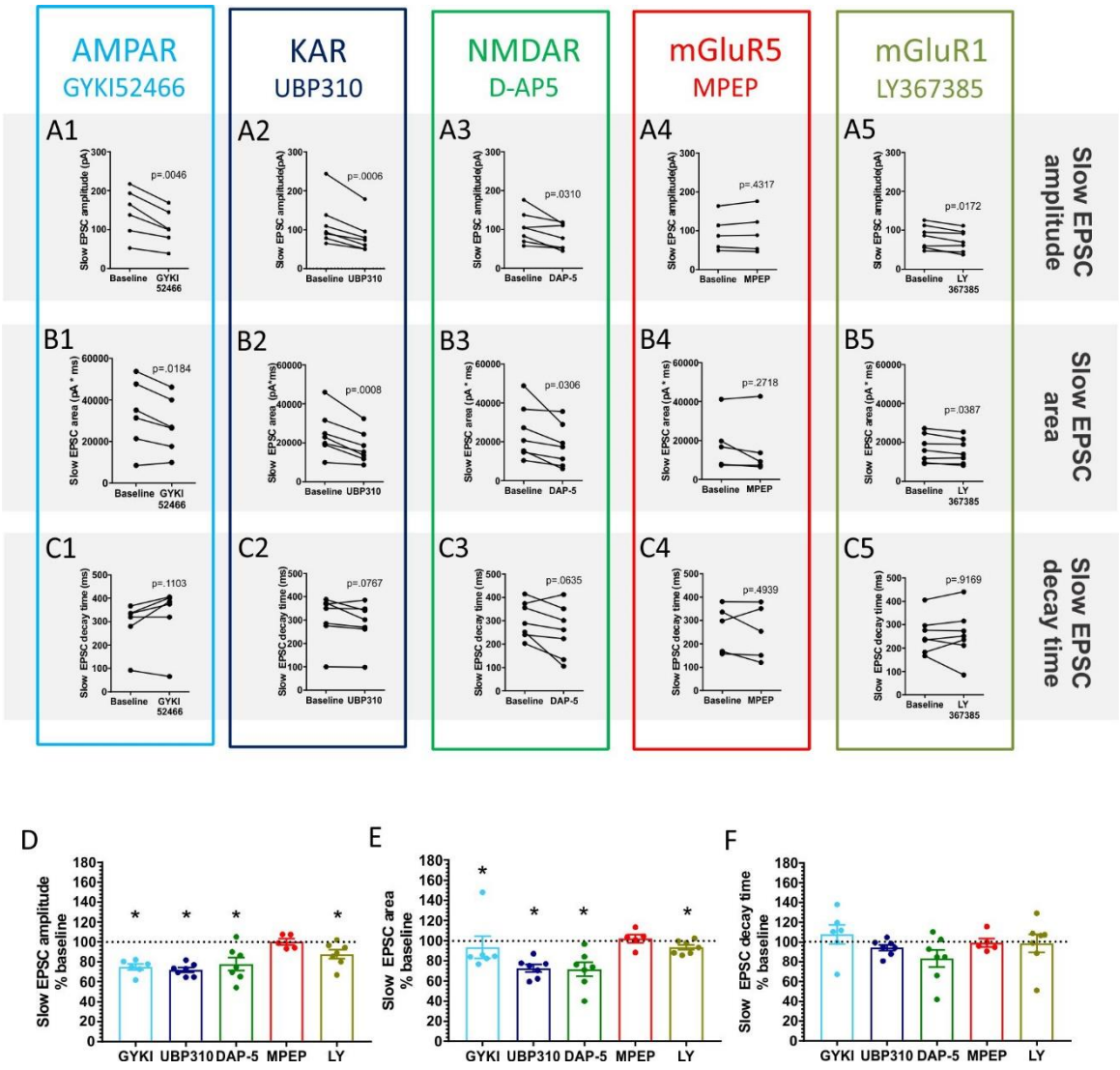

Fig 5. Slow EPSCs are mediated by a combination of ionotropic glutamate receptors in MCH neurons.

Top: Raw values are shown for slow EPSC amplitude **(A1-A5),** area **(B1-B5),** and decay time **(C1-C5).** Each connected set of two data points represents one MCH neuron before and during glutamate receptor antagonists.
Bottom: Data is grouped and shown as percent baseline to compare the relative contribution of each glutamate receptor **(D-F).** *p<0.05 vs. baseline.

3-3 Evoked fast and slow EPSCs are differentially impacted by glutamate transporter blockade

We next wanted to investigate how glutamate transporters influence excitatory transmission in MCH neurons. Thus, the effects of glutamate transporter blockers were tested on evoked EPSCs using 20 pulse x 50 Hz train stimulation, similarly to Figure 3. After a stable baseline had been established, the non-specific transporter inhibitor TFB-TBOA (5 µM) or the GLT-1 specific inhibitor DHK (100 µM) was bath applied for 5 minutes (refer to section 3-4 for rationale behind concentrations used). Representative superimposed traces show a large shift in baseline during glutamate transporter blockade (Fig 6A,B; arrows) that was reversible after washing. When this shift in baseline current is removed and traces are aligned at the baseline (Fig 6C,D) EPSCs are flattened in the presence of TFB-TBOA (Fig 6C), while EPSCs are still present during DHK (Fig 6D). Subtracted traces (Fig 6E,F) illustrate the current sensitive to the glutamate transporter inhibitor used. The TFB-TBOA subtracted trace (Fig 6E) is much larger than the DHK subtracted trace (Fig 6F) indicating that TFB-TBOA eliminates more evoked EPSCs than DHK does.

We analyzed the fast EPSC amplitude relative to its own baseline immediately preceding the stimulus artifact. This revealed that fast EPSC amplitude was significantly decreased in the presence of TFB-TBOA (paired t test, $t(4) = 3.25$; $p = 0.0313$; n = 5 cells, n = 3 rats; Fig 7A2). Fast EPSC amplitude diminished quickly and did not reverse to baseline levels even with a prolonged wash (Fig 7A1). Conversely, fast EPSC amplitude remained stable throughout DHK application (paired t test, $t(5) = 1.39$; $p = 0.2218$; n = 6 cells; n =

3 rats; Fig 7B1,B2).. These results indicate that fast EPSCs are occluded when all glutamate transporters are blocked by TFB-TBOA, but not affected when GLT-1 alone is blocked by DHK (unpaired t test, $t(9) = 11.21$; $p = 0.0001$; Fig 7C). The difference in the effect of the two blockers suggests a role for glutamate transporters other than GLT-1.

Next, we analyzed the slow EPSC in the same set of cells. In contrast to the fast EPSC results, DHK significantly decreased the slow EPSC amplitude (paired t test, $t(5) = 4.91$; $p = 0.0044$; Fig 8C1,C2) and slow EPSC area (paired t test, $t(5) = 6.07$; $p = 0.0018$; Fig 8D1,D2). Interestingly, TFB-TBOA induced a biphasic effect on slow EPSC amplitude with an increase followed by a decrease (Fig8A1). The initial increase was consistently observed among cells; however, this could be due to the rapid downward shift in the baseline induced by the transport blocker (to be addressed below) rather than a real increase in EPSC amplitude. Once the baseline stabilized, a significant decrease in slow EPSC amplitude was observed (paired t test, $t(4) = 3.35$; $p = 0.0285$; Fig 8A2). This did not accompany a significant change in the slow EPSC area (paired t test, $t(4) = 1.70$; $p = 0.1629$; Fig 8B2), which could be due to a dramatic inhibition of slow EPSC, which made it difficult to reliably measure the slow EPSC area.

Together we have shown that the fast and slow components of EPSCs are differentially affected by glutamate transporter blockade. TFB-TBOA occludes fast EPSCs more than DHK however, DHK decreases slow EPSC parameters more consistently than TFB-TBOA. These results suggest an important role for GLT-1 and non GLT-1 transporters, namely GLAST and EAAC1.

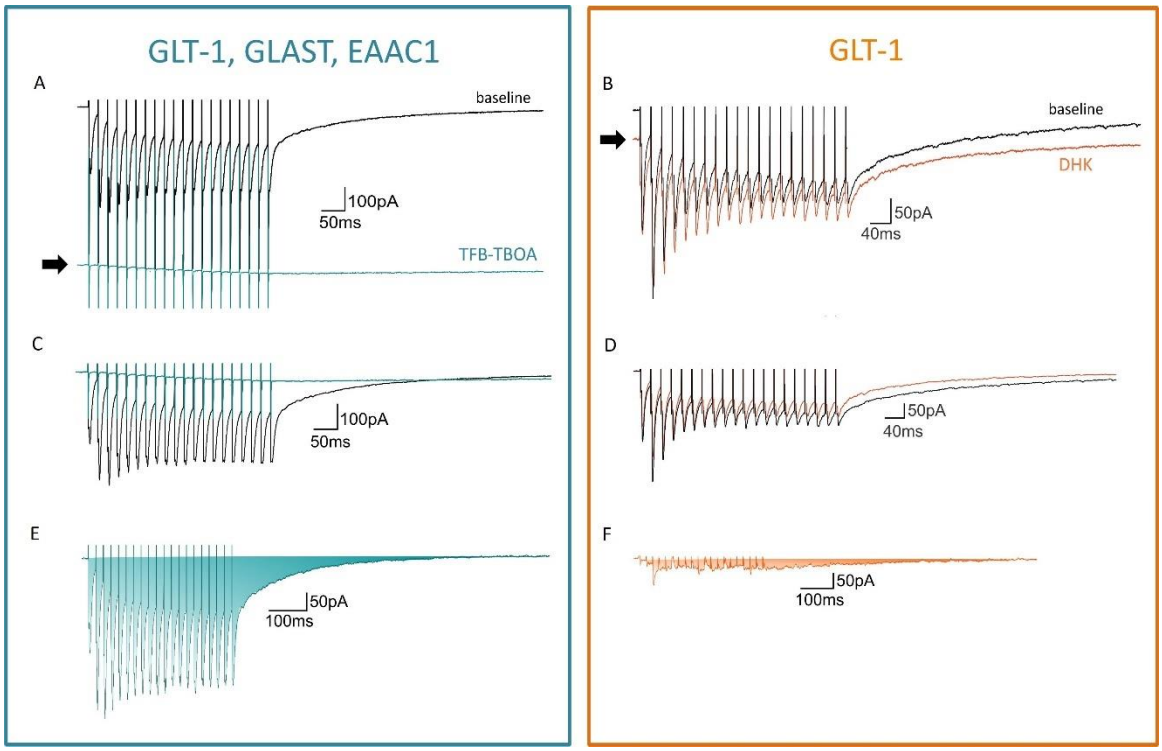

Fig 6. Effect of glutamate transporter blockade on evoked biphasic EPSCs in MCH neurons.

Left: green box contains traces during TFB-TBOA which inhibits GLT-1, GLAST and EAAC1. **Right:** orange box contains traces during DHK which inhibits GLT-1.
A,B) Representative averaged traces of biphasic EPSCs evoked by train stimulation recorded from individual MCH neurons during baseline (black traces) and during glutamate transporter blockade (colored traces). Arrows indicate the shift in baseline holding current during **A)** TFB-TBOA (5µM) and **B)** DHK (100µM) application.
C,D) Superimposed traces have been aligned at the baseline to illustrate the effect on evoked biphasic EPSCs during glutamate transporter blockade. EPSCs appear flattened during TFB-TBOA **(C)** but still present during **(D)** DHK
(E,F). Subtracted traces indicate the difference between the responses to synaptic stimulation with and without the transporter blocker, representing the current sensitive to either TFB-TBOA **(E)** or DHK **(F).** Note that these traces do not account for the tonic shift in baseline holding current due to the transporter blockers.

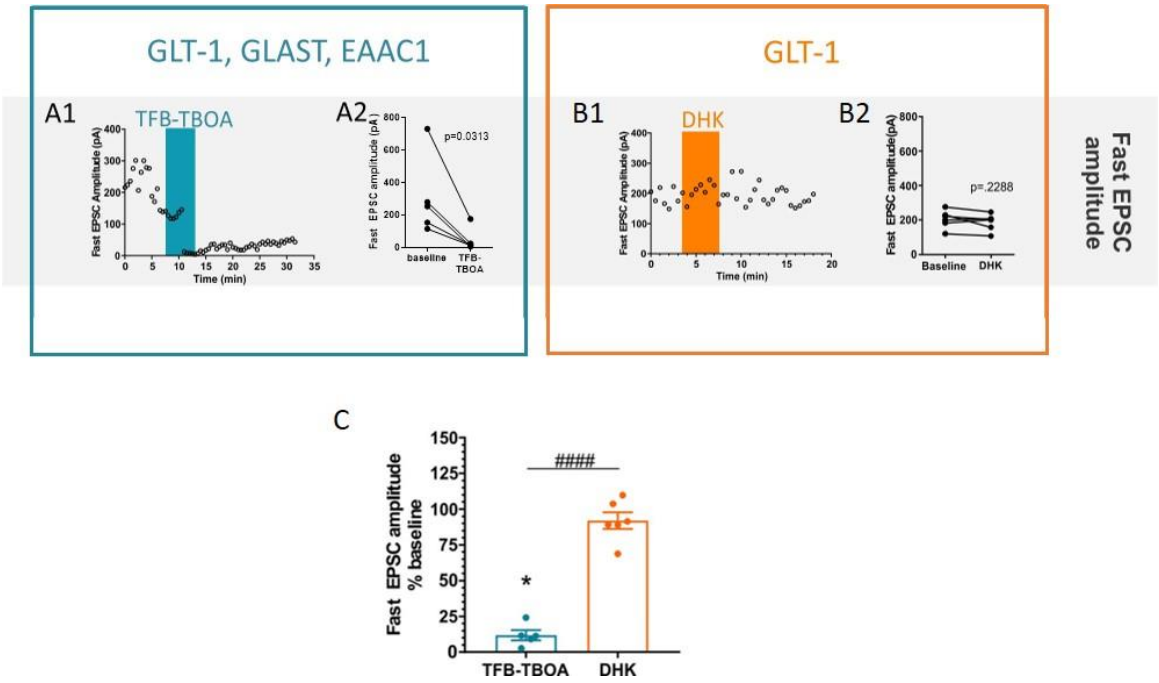

Fig 7. Evoked fast EPSCs are eliminated by TFB-TBOA but not by DHK.

Left: green box contains traces during TFB-TBOA which inhibits GLT-1, GLAST and EAAC1. **Right:** orange box contains traces during DHK which inhibits GLT-1.
A) Representative time effect plots and summary graphs depicting the effect of TBOA on fast EPSC amplitude **(A1, A2)**. TBOA application is indicated in time-effect plots with green boxes.
B) Representative time effect plots and summary graphs depicting the effect of DHK on fast EPSC amplitude (**B1, B2).** DHK application is indicated in time-effect plots with orange boxes.
C) Data is grouped and shown as percent baseline to compare the relative contribution of each glutamate transporter inhibitor. #### $p<0.0001$, TBOA vs DHK; *$p<0.05$ vs. baseline.

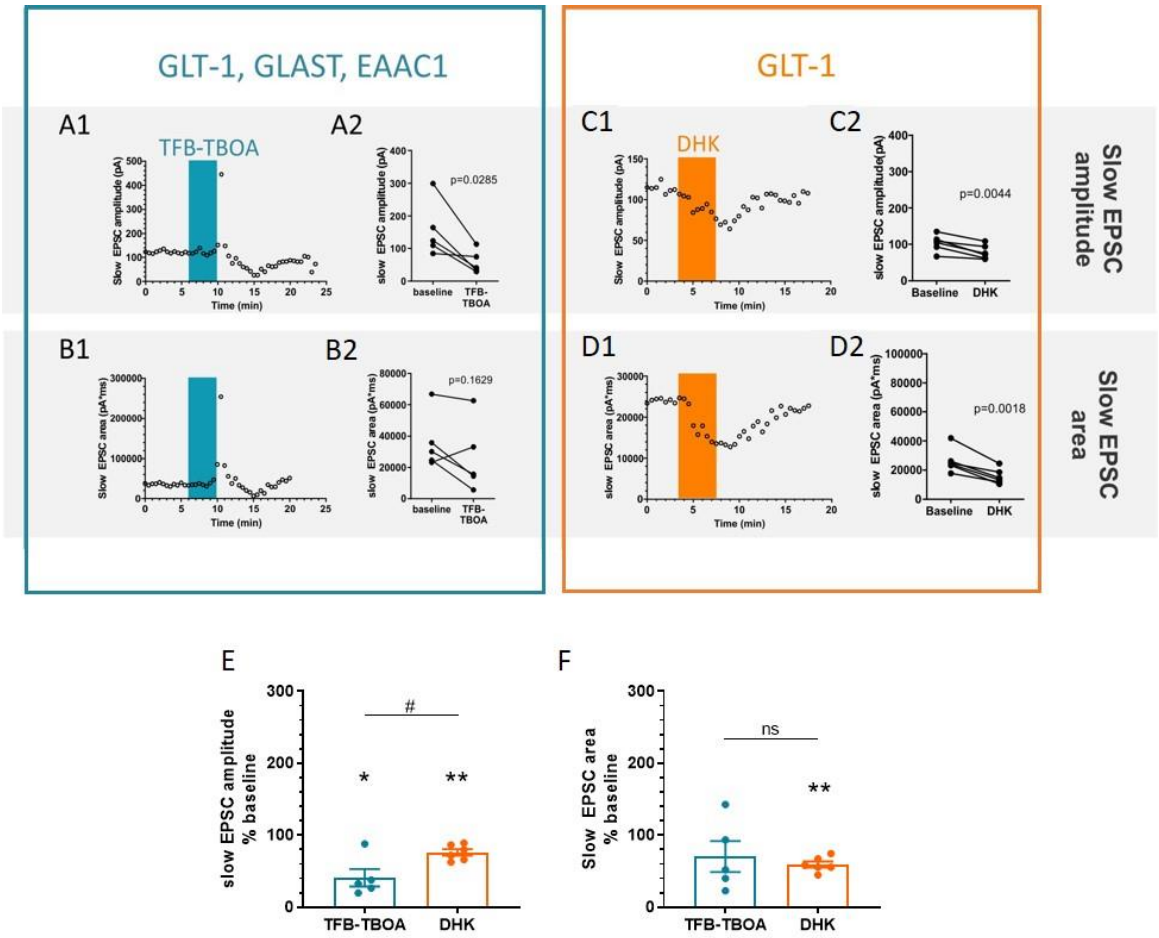

Fig 8. TFB-TBOA induces biphasic effect on evoked slow EPSC in MCH neurons.

Left: green box contains traces during TFB-TBOA which inhibits GLT-1, GLAST and EAAC1. **Right:** orange box contains traces during DHK which inhibits GLT-1.
A-B) Representative time effect plots and summary graphs depicting the effect of TBOA on slow EPSC amplitude **(A1, A2)**, slow EPSC area (**B1, B2).** TBOA application is indicated in time-effect plots with green boxes.
C-D) Representative time effect plots and summary graphs depicting the effect of DHK on slow EPSC amplitude **(C1, C2)** and slow EPSC area (**D1,D2**). DHK application is indicated in time-effect plots with orange boxes.
E-F) Data is grouped and shown as percent baseline to compare the relative effect of each glutamate transporter inhibitor. # $p<0.05$ TBOA vs DHK; *$p<0.05$ vs. baseline.

3-4 Glutamate transporter blockade induces tonic current in MCH neurons

During glutamate transporter blockade, we observed robust, tonic inward currents in MCH neurons. Thus, we next turned our attention to these tonic currents. We found that a 5 minute application of TFB-TBOA resulted in a large tonic current in MCH neurons (Fig 9A). Interestingly, this tonic current was reversible upon wash, which is distinct from the effect on evoked fast EPSCs that did not reverse even with prolonged washout (Fig 7A1). This TFB-TBOA effect was found to be concentration dependent, with 10 µM application inducing a maximal current approximately twice the amplitude of the 5 µM application (one way ANOVA, $F(3, 25) = 11.43$, $p < 0.0001$; Tukey's test for TFB-TBOA 5 µM vs 10 µM $p = 0.0012$; Fig 9B). The higher concentrations often resulted in incomplete washout of the tonic current or unstable recording, therefore, we decided to use 5 µM TFB-TBOA for the remaining TFB-TBOA experiments. These results confirm that non-specific glutamate transporter blockade leads to tonic current in MCH neurons.

TFB-TBOA is a non-specific glutamate transporter blocker, therefore it blocks all known transporters expressed in the hypothalamus: namely GLT-1 and GLAST (expressed on astrocytes) and EAAC1 (expressed on neurons). In order to determine how each of these three types of transporters of interest contributes to regulating tonic current in MCH neurons, we next decided to test the specific inhibitor of astrocytic glutamate transporter GLT-1, DHK. We found that 5 minute application of DHK induced a reversible tonic current in MCH neurons (Fig 9C). The two cells in the 300 µM group displayed currents comparable to those of greatest magnitude in the 100 µM group (Fig 9D). This suggests

that 100 µM is near saturating, and thus this concentration was used for the remainder of DHK experiments.

Next, we tested the GLAST specific inhibitor, UCPH101. Application of UCPH101 (50-100 µM) induced no tonic current at concentrations previously shown to effectively block GLAST (Abrahamsen et al., 2013) when applied for 5-15 min (Fig 9E,F). Additionally, UCPH101 had no additive effect when combined with 100 µM DHK (one way ANOVA $F(3,33) = 126.6$, $p < 0.0001$; Tukey's test for DHK vs. DHK + UCPH101 $p > 0.9999$; Fig 9G), confirming that GLAST is not involved in regulation of basal excitatory transmission to MCH neurons. With GLAST no longer being considered as a contributor, the significant discrepancy between the TFB-TBOA-induced and the DHK-induced tonic currents suggests a likely role of the neuronal transporter EAAC1 in regulating tonic current in MCH neurons (one way ANOVA $F(3,33) = 126.6$, $p < 0.0001$; Tukey's test for TFB-TBOA vs DHK $p < 0.0001$; Fig 9G).

Interestingly, we also observed that the tonic current induced by TFB-TBOA was not always smooth and typically included "stepwise currents" (i.e. rapid downward shifts in current ranging from 50-150 pA in size; Fig 9A, arrows). Note that these stepwise currents were only observed with TFB-TBOA and not the other transporter inhibitors tested.

3-5 Tonic Currents are induced by ambient glutamate

As previously mentioned, tonic excitatory currents are often induced by ambient levels of glutamate in the extracellular space. Many factors can influence ambient glutamate levels such as neuronal and non-neuronal release, and glutamate transporter activity.

Here, we wanted to determine the source of glutamate responsible for the tonic current in MCH neurons. Since the majority of neuronal release of glutamate depends on Na+ spikes, we used TTX, a sodium channel blocker that prevents action potential dependent vesicular release of neurotransmitter. We found that TTX had no significant effect on the amplitude of tonic currents induced by TFB-TBOA (5 µM) (unpaired t test, $t(20) = 1.68$; $p = 0.1083$; n = 13 cells, n = 8 rats for TFB-TBOA; n = 9 cells, n = 5 rats for TTX + TFB-TBOA; Fig 10A) or DHK (100 µM) (unpaired t test, $t(22) = 0.125$; $p = 0.9010$; n = 16 cells, n = 13 rats for DHK; n = 8 cells, n = 7 rats for TTX + DHK; Fig 10B). This suggests that these tonic currents do not depend on the action potential-dependent neuronal release of glutamate, rather they are likely induced by buildup of spontaneously released glutamate or ambient glutamate from non-neuronal sources.

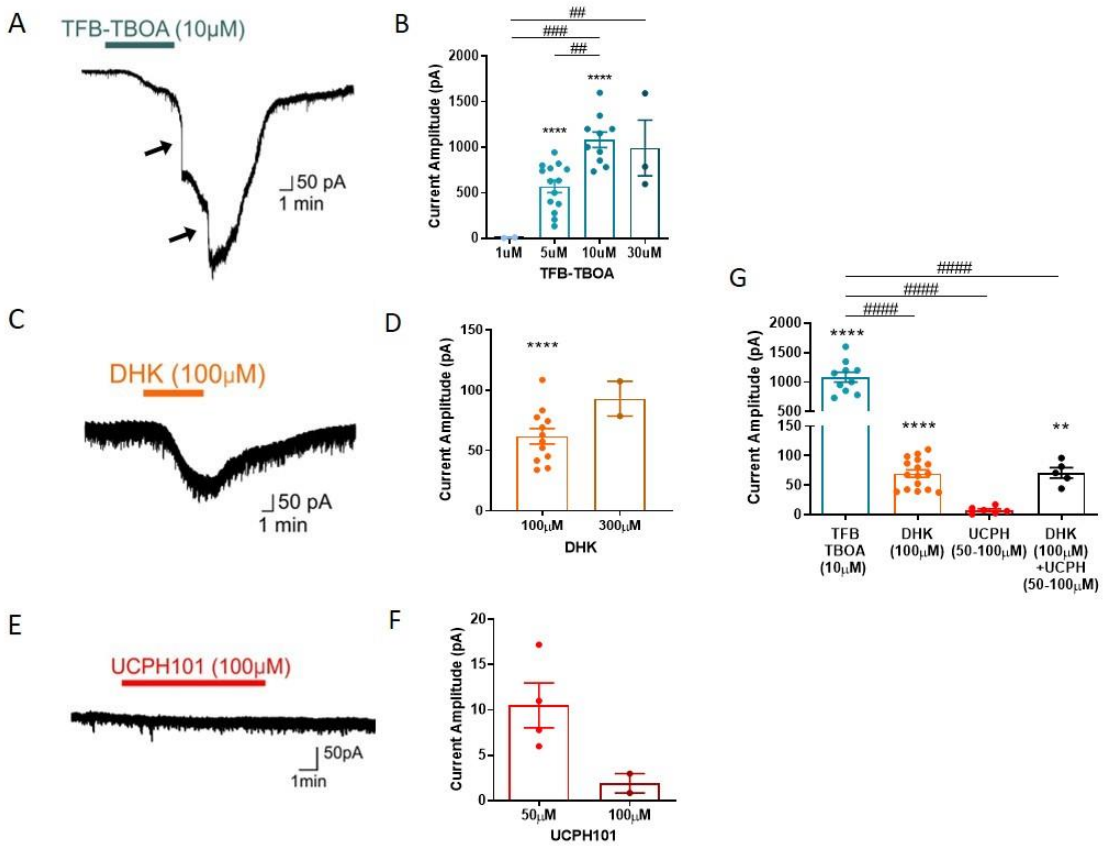

Fig 9. Glutamate transporter blockade induces tonic current in MCH neurons.

A) Representative voltage clamp trace illustrating the large, reversible inward current induced by the non-specific transporter inhibitor TFB-TBOA. Arrows indicate stepwise currents. **B)** TFB-TBOA induced effect is concentration dependent. **C)** Representative voltage clamp trace illustrating the reversible, inward current induced by the GLT-1 specific inhibitor DHK. **D)** DHK induces similar effects at 100 or 300μM. **E)** Representative voltage clamp trace illustrating a lack of effect of the GLAST specific blocker UCPH101. **F)** Blockade of GLAST with UCPH101 had no effect at either 50 or 100μM. UCPH101 was applied for 5-15 min, which yielded similar effect, thus the results were combined. **G)** Data is grouped to compare the amplitudes of tonic current between the different transporter inhibitors used. ##p<0.05, ###p<0.001, ####p<0.0001; **p<0.01, ***p<0.001, ****p<0.0001 vs baseline.

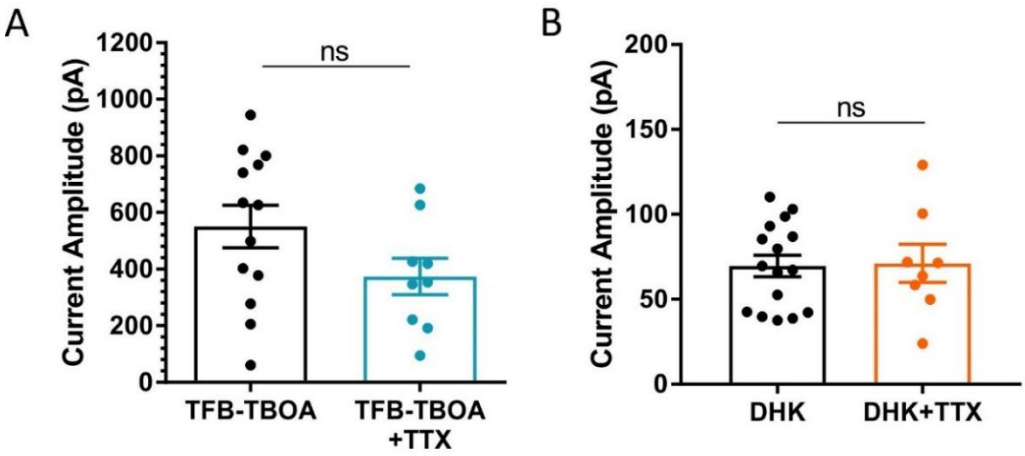

Fig 10. Tonic current is induced by ambient glutamate.

TTX (1µM), a sodium channel blocker that prevents action potential dependent release of neurotransmitter does not affect tonic currents induced by either **A)** TFB-TBOA (5µM) or **B)** DHK (100µM). These data indicate that tonic currents regulated by glutamate transporters do not depend on action potential-dependent presynaptic release of glutamate.

3-6 TBOA induced tonic current is mediated primarily by NMDARs

We found that the non-specific transporter inhibitor TFB-TBOA induced a large, tonic, reversible current in MCH neurons (see Fig 9A). In order to determine which glutamate receptor(s) were responsible for mediating this TFB-TBOA induced effect, we tested a series of iGluR and mGluR antagonists. When the NMDAR antagonist DAP5 (50μM) was present in the bath, the amplitude of the TFB-TBOA induced current was significantly reduced (one way ANOVA $F(5,46) = 3.27$, $p = 0.013$; Dunnet's test for TFB-TBOA vs DAP5 $p = 0.0018$; all other Dunnet's comparisons $p > 0.05$; Fig 11A,B). In contrast, the AMPAR antagonist GYKI52466, the KAR antagonist UBP310 and the group I mGluR antagonists MPEP and LY367385 had no significant effect. This indicates that it is NMDARs mediating the majority of the TFB-TBOA induced current.

3-7 DHK induced tonic current is mediated by KARs

We found that the GLT-1 specific inhibitor DHK induced a tonic, reversible current in MCH neurons (see Fig 9C). In order to determine which glutamate receptor(s) were responsible for mediating this DHK induced effect, we tested glutamate receptor antagonists. A previous study in our laboratory found that the non-NMDAR antagonist DNQX largely blocked the DHK effect, but not the AMPAR specific antagonist or the group I mGluR antagonists, suggesting that KAR may play an important role. Here, we tested the KAR specific antagonist UBP310 (10μM) and found that it abolished the DHK-induced tonic current (unpaired t test, $t(12) = 5.62$, $p = 0.0001$; $n = 6$ cells, $n = 2$ rats for DHK alone; $n = 8$ cells, $n = 5$ rats for UBP310+DHK; Fig 12A,B). These results indicate that KAR mediate the DHK current.

Taken together, these results suggest that EAAC1 may regulate NMDAR activation while GLT-1 tightly controls KAR activation by ambient glutamate.

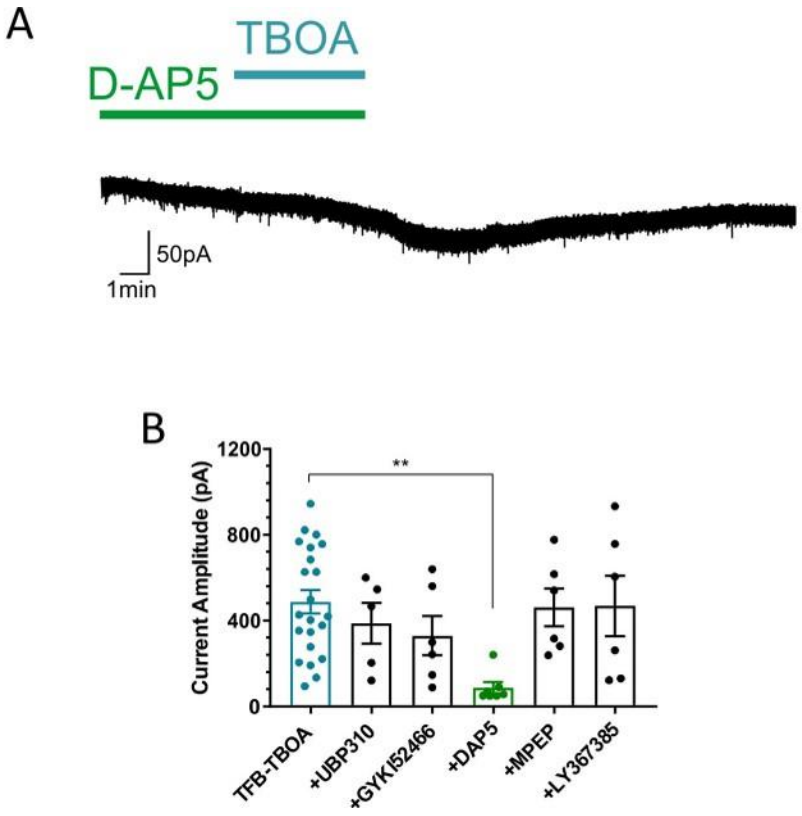

Fig 11. Glutamate transporters control NMDAR activation by ambient glutamate.

A) Representative voltage clamp trace illustrating the TFB-TBOA-induced effect (see Fig 9A) is largely attenuated by the NMDAR antagonist D-AP5 (50µM).
B) Grouped data summarizing the effect of glutamate receptor antagonists on the TFB-TBOA induced current. The amplitude of the TFB-TBOA-induced tonic current is significantly reduced by D-AP5, but not by other glutamate receptor antagonists.
**p<0.01.

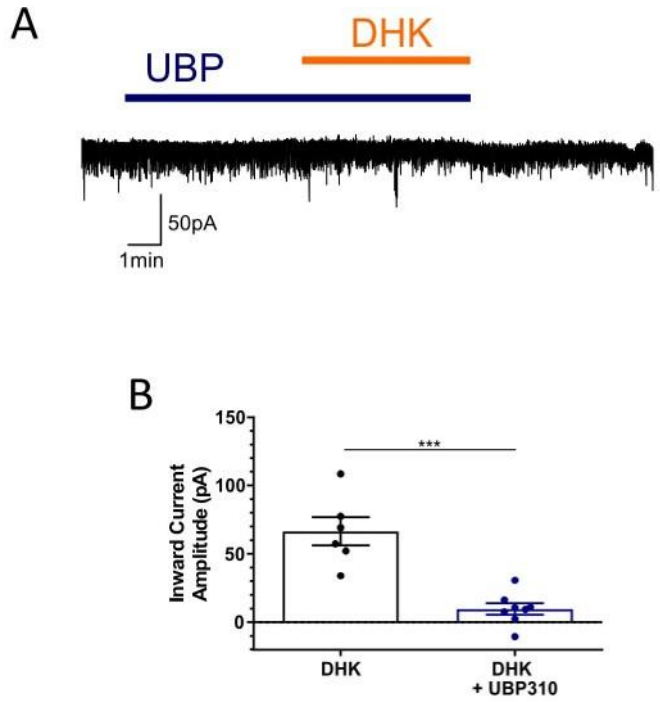

Fig 12. GLT-1 tightly controls KAR activation by ambient glutamate.

A) Representative voltage clamp trace illustrating the DHK induced effect (see Fig 9C) when the KAR antagonist UBP310 (10μM) is present in the bath.
B) The amplitude of the DHK-induced tonic current is significantly reduced by UBP310. This indicates that UBP310 leads to complete blockade of DHK induced tonic current. ***$p<0.001$.

4-0 Discussion

In the present study, we have shown that MCH neurons display biphasic EPSCs consisting of both fast and slow components. These fast and slow phases of EPSC were found to be mediated by distinct glutamate receptors types. We also found that blockade of glutamate transporters leads to a reversible, tonic current in MCH neurons likely induced by ambient glutamate from a non-neuronal source. The size of the tonic current is dependent on the concentration and specificity of the inhibitor used; therefore, we can deduce which transporter types are involved in glutamate clearance and the regulation of excitatory transmission in MCH neurons.

4-1 GLT-1

GLT-1 is highly enriched at the cell surface in astrocytes and is estimated to be responsible for up to 90% of glutamate reuptake in the forebrain (Holmseth, 2012; Vandenburg & Ryan, 2013). We found that blockade of GLT-1 by DHK induced a tonic current in MCH neurons indicating that GLT-1 actively clears glutamate at these cells. The TFB-TBOA induced tonic current was found to be significantly larger than the DHK induced tonic current. As TFB-TBOA is a non-specific inhibitor blocking all transporter types, while DHK only blocks GLT-1, our results indicate that in addition to GLT-1, other transporters such as EAAC1 and GLAST can also actively clear glutamate around MCH neurons.

4-2 GLAST

UCPH101 has been shown to bind noncompetitively to GLAST, inducing a long lasting state of inhibition. (Abrahamsen et al., 2013). However, we found that the GLAST specific inhibitor UCPH101 had no effect on tonic current at the two concentrations tested (50-100uM). This result was unexpected as GLAST is known to be expressed on the surface of astrocytes throughout the CNS with the greatest density in the cerebellar cortex and relatively high densities in the hippocampus and the hypothalamus (Schmitt et al., 1997). Schmitt et al. (1997) reported that hypothalamic GLAST expression decreased from the medial to the lateral areas which may explain our findings as our recording was mostly performed in the lateral area than in the medial area. Further, UCPH101 was ineffective even when combined with DHK, excluding the possibility that GLT-1 compensated for the lack of GLAST activity. These results strongly suggest that GLAST is not present or not active at MCH neurons in basal conditions. This means that the significant discrepancy between the TFB-TBOA induced and the DHK induced tonic current cannot be due to GLAST and is likely due to the neuronal transporter EAAC1. If this is true, then EAAC1 would be responsible for the majority of glutamate clearance at MCH neurons.

4-3 EAAC1

Compared to astrocytic GLT-1 and GLAST which are enriched at the cell surface, EAAC1 immunolabelling is mostly intracellular with only 30% of the protein localized to the plasma membrane (Holmseth et al., 2012). Further, overall EAAC1 expression levels are significantly lower than astrocytic glutamate transporters. Based on these differences,

it has been suggested that EAAC1 cannot have an appreciable effect on glutamate clearance in the brain.

It has been proposed that EAAC1 participates indirectly in the regulation of neurotransmission by serving as a glutamate buffer (i.e. EAAC1 repeatedly binds and unbinds glutamate rather than participating in rapid transport.(Scimemi et al., 2009; Holmseth et al., 2012). Buffering prolongs the glutamate transient by slowing its clearance by astrocytic transporters which are expressed in high densities surrounding the synapse (Danbolt, 2001; Scimemi et al., 2009). Indeed, EAAC1 KO models display faster glutamate clearance without any change to the overall uptake capacity of astrocytes (Scimemi et al., 2009). This supports the idea that EAAC1 plays a distinct role in excitatory transmission through buffering of synaptic glutamate (Scimemi et al., 2009; Holmseth et al., 2012). Interestingly, EAAC1 has been shown to regulate extracellular glutamate concentrations without altering synaptic receptor activation, suggesting that EAAC1 prevents diffusion and spillover (Scimemi et al., 2009). Diamond et al. (2001) report that EAAC1 limits NMDAR activation by glutamate spillover. Further, EAAC1 KO display enhanced NMDAR activation (Scimemi et al., 2009). As EAAC1 is not enriched in dendritic spines (Holmseth et al., 2012) this suggests that EAAC1 is localized outside of the synapse and regulates glutamate diffusion to perisynaptic/extrasynaptic receptors, namely NMDARs. Extrasynaptic receptor activation by spillover/diffusion typically has a slower time course than synaptic receptor activation, therefore, this may explain our findings indicating an important role for EAAC1 in regulation of ambient glutamate and tonic current in MCH neurons.

The lack of consensus regarding the role of EAAC1 is in large part because there are no specific pharmacological tools to target EAAC1. We attempted to block EAAC1 using an antibody targeting the intracellular portion of the transporter. The antibody was added to the internal patch pipette solution (50-100ug/mL) and permitted to diffuse into the cell for up to 30 minutes while the holding current was recorded. Preliminary results (data not shown) show that any tonic current recorded with the antibody is not significantly different than the average drift in holding current during a typical patch clamp recording over a 30-min period. This suggests that EAAC1 expressed by the postsynaptic cell is not responsible for the tonic currents in MCH neurons. However, without a positive control we are unsure whether the antibody had the intended effect of functionally blocking EAAC1. Therefore, more testing is needed to determine the exact contribution of EAAC1 in these cells.

4-4 Transporter inhibition on evoked EPSCs

TFB-TBOA induced a large tonic current while simultaneously eliminating evoked EPSCs within minutes of application. Transporter blockade increases extracellular glutamate levels within seconds (Danbolt, 2001), therefore, it is likely that glutamatergic receptors are completely saturated during TFB-TBOA. At this time, any additional transmitter released by synaptic stimulation would have an insignificant contribution to the already maximal extracellular glutamate levels. This could explain why evoked EPSCs are completely flattened during TFB-TBOA. Alternatively, the extreme glutamate flooding observed during TFB-TBOA may activate presynaptic group II and group III

mGluRs which are known to have an inhibitory effect on glutamate release (Niswender and Conn, 2010). These possibilities are not exclusive of each other.

DHK induced a smaller tonic current during which evoked EPSCs remained largely intact but had different impact on fast and slow EPSCs. Fast EPSCs were unaffected by DHK suggesting that GLT-1 preferentially clears ambient rather than synaptic glutamate. During DHK, EAAC1 is functionally available which may explain why fast EPSCs are unchanged. Interestingly, the slow EPSC was reduced during DHK and returned to baseline during the wash. We expected that the slow EPSC would have increased in the absence of GLT-1 due to slower clearance of synaptic glutamate. However, it is possible that slow EPSCs represent glutamate spillover and activation of extrasynaptic receptors. If so, ambient glutamate and spillover glutamate may be competing for the same receptors. As DHK increases ambient glutamate that would occupy extrasynaptic receptors, this could occlude the effect of glutamate spilling over from synapses, explaining the reduction in slow EPSCs.

4-5 Ambient glutamate mediates tonic current

Research suggests that tonic currents are typically induced by ambient glutamate, the low basal level of transmitter present in the extracellular space (Le Meur et al., 2007). We found that both the DHK and TFB-TBOA induced tonic currents were not blocked by TTX, suggesting that this current does not rely on action potential dependent neuronal

release of glutamate. Instead, tonic current is likely induced by ambient glutamate from a non-neuronal source in MCH neurons.

These persistent tonic currents have been observed in various cell types and are often mediated by extrasynaptic NMDARs (Le Meur et al., 2007; Povysheva and Johnson, 2012; Papouin and Oliet, 2014). Our TFB-TBOA induced tonic current was found to be primarily mediated by NMDARs which agrees with previous reports. On the other hand, our DHK induced tonic current was found to be mediated exclusively by KARs.

4-6 Biphasic EPSC in MCH

MCH neurons display a biphasic EPSC, similar to other cells such as hippocampal interneurons, Renshaw cells of the spinal cord and thalamic recticular nucleus neurons (d'Incamps et al., 2012; Sun et al., 2013; Stincic and Frerking, 2015). However, this is not common as orexin neurons, another lateral hypothalamic cell group intermingled with MCH neurons, do not show slow EPSCs (Briggs et al. 2018). In cells that show the slow phase of EPSC, it is often mediated by mGluRs or KARs (Castillo et al., 1997; Sheng et al., 2017), but also by AMPARs in cerebellar unipolar brush cells and CA1 hippocampal interneurons (Stincic and Frerking, 2015; Zampini et al., 2016). EPSCs on a slow timescale are typically induced by stimulation trains causing buildup and entrapment of glutamate in the synaptic cleft (Bertrand and Galligan, 1994; Zampini et al., 2016). Receptors mediating the slow EPSC may be located further from the site of release serving to sense glutamate spillover (Zampini et al., 2016). Further, distinct subunit makeup of receptors that have fast or slow kinetics may determine their contribution to

fast and/or slow EPSCs (Zampini et al., 2016). The presence of the slow EPSC in MCH neurons may provide greater diversity in excitatory signaling and functionally important regulation of homeostatic mechanisms such as sleep wake states and energy homeostasis.

4-7 AMPARs

AMPARs are well established as typical mediators of fast EPSCs and our finding is consistent with this (Jonas, 2000; Wondolowski and Frerking, 2009). While AMPARs were the major contributor to fast EPSCs in MCH neurons, they also had a small contribution to slow EPSC. Distinct subunit makeup of receptors can determine their various roles in neurotransmission. Stincic & Frerking (2015) report that AMPARs mediate biphasic EPSCs in CA1 hippocampal interneurons and this is dependent on the GluA2 subunit. Specifically, GluA2 containing AMPARs mediate fast EPSCs while GluA2 lacking AMPARs mediate slow EPSCs (Stincic and Frerking, 2015). Perhaps MCH neurons express both GluA2 containing and GluA2 lacking AMPARs which explains their contribution to the biphasic EPSC.

4-8 KARs

KARs have been previously identified as key mediators of slow EPSCs in various cell types (Castillo et al., 1997; Lerma, 2003; Wondolowski and Frerking, 2009). Consistent with this, our findings show that KARs mediate the slow EPSC as well as a small portion of the fast EPSC in MCH neurons. In contrast to EPSCs, the DHK-induced tonic current was found to be exclusively mediated by KARs. Further, the DHK induced tonic current is independent of synaptically released glutamate because it is insensitive to the Na+

channel blocker TTX. Recall that fast EPSCs were unaffected during DHK, suggesting that GLT-1 regulates ambient rather than synaptic glutamate. Together, these findings support the inference that KARs are located extrasynaptically and are only activated by ambient glutamate or synaptic spillover diffusing farther into the extracellular space.

4-9 NMDARs

Extrasynaptic NMDARs have been found to mediate tonic currents in various cell types including CA1 hippocampal neurons and pyramidal cells of the prefrontal cortex (Le Meur et al., 2007; Povysheva and Johnson, 2012). Similarly, our findings based on a pharmacological study suggest that NMDARs are the major mediator of tonic current in MCH neurons. NMDARs were also found to be the greatest contributor to slow EPSC while not contributing to fast EPSCs at all. However, the involvement of NMDARs was puzzling to us, as all experiments were conducted at the holding potential of -70 mV, which would argue against the involvement of NMDARs due to the channel pore Mg2+ block. Perhaps this can be explained by a space clamp error, whereby NMDARs expressed on distal dendrites are likely to escape the somatic voltage clamp system. If this is the case, removing Mg^{2+} should permit the activation of more NMDAR, resulting in larger tonic current. To test this idea, identical experiments were performed using Mg-free ACSF. The presence or absence of Mg^{2+} did not appear to influence NMDARs ability to mediate the TFB-TBOA induced tonic current (i.e. TFB-TBOA tonic current was similar in the presence or absence of Mg^{2+} in ACSF. Thus, NMDARs may be involved in tonic currents in an unconventional way, such as a metabotropic signaling mechanism that does not require the ion channel (Weilinger et al., 2016).

4-10 mGluR1 & mGluR5

Group 1 mGluRs have been found to mediate slow EPSCs in various cell types such as CA3 hippocampal interneurons and cerebellar Purkinje cells (Hirono et al., 1998; Eguchi et al., 2016). Specifically in MCH neurons, it has been reported that the slow EPSC is mediated through mGluR5 (Huang and van den Pol, 2007). However, to our surprise the mGluR5 antagonist MPEP had no effect on the slow EPSC or fast EPSC in the present study. Conversely, we found that the mGluR1 antagonist decreases both fast and slow EPSC while increasing the PPR, suggesting a presynaptic mechanism for altering glutamate release. Group I mGluRs are typically expressed postsynaptically, therefore the observed decrease in fast EPSC could be explained by a retrograde messenger (Niswender and Conn, 2010). Alternatively, mGluR1 could be expressed presynaptically.

4-11 Predicted subcellular location of receptors and transporters in MCH neurons

Based on the findings described in this thesis, we propose the following subcellular localization of glutamate receptors and transporters (Fig 13). We have demonstrated that glutamate transporters GLT-1 and EAAC1, but not GLAST, are actively clearing glutamate around MCH neurons. GLT-1 seems to regulate ambient glutamate concentrations at extracellular receptors; thus we speculate that GLT-1 will be expressed on astrocytic processes at extrasynaptic sites. EAAC1 likely regulates ambient glutamate at perisynaptic/extrasynaptic receptors by preventing spillover and may also prevent re-entry of glutamate back into the synaptic cleft (Scimemi et al., 2009). EAAC1 is primarily found in the soma and dendrites but is not concentrated in dendritic spines,

therefore, it is unlikely to be highly localized to the synapse depending on the types of synaptic contacts formed (axodendritic, axosomatic, axoaxonic) (Holmseth et al., 2012). We speculate that EAAC1 will be expressed at perisynaptic/extrasynaptic sites where it can directly prevent activation of extrasynaptic NMDARs by ambient glutamate (Trotti et al., 1998).

Our results suggest that in MCH neurons, AMPARs are the major mediator of fast EPSCs and are likely expressed within the core of the PSD directly opposing vesicular release sites, consistent with the literature (Jonas, 2000; Scheefhals and MacGillavry, 2018). NMDARs significantly contributed to the slow EPSC; hence, these receptors are likely expressed perisynaptically and activated by synaptic spillover. Our findings suggest that NMDARs do not contribute to fast EPSCs, therefore, we expect that their expression within the synapse is minimal, although it would be necessary to confirm this under a condition in which NMDARs are relieved of Mg^{2+} block. NMDARs were also found to mediate the majority of the TFB-TBOA induced tonic current, suggesting these receptors are expressed at extrasynaptic sites and activated by extreme glutamate flooding. While extrasynaptic NMDARs have been viewed as a "reserve pool" simply waiting to be recruited to active synapses, these clusters may serve a unique signaling function independent of synaptic receptors (Papouin and Oliet, 2014). KARs are the exclusive mediators of the DHK induced tonic current while also contributing to both fast and slow EPSC, thus these receptors may be expressed at synaptic, perisynaptic and extrasynaptic locations. mGluRs are typically located in the perisynaptic zone and activated by synaptic glutamate spillover (Huang et al., 2004). Thus mGluR1, which exhibited a minor

contribution to the slow EPSC, is likely expressed perisynaptically. Since mGluR1 inhibition also increased PPR indicating reduced release probability, it could also trigger retrograde signaling or be expressed presynaptically. mGluR5 does not appear to contribute to excitatory currents in MCH neurons so if these receptors are expressed at these synapses, they may be involved in second messenger signaling pathways independent of ionic currents.

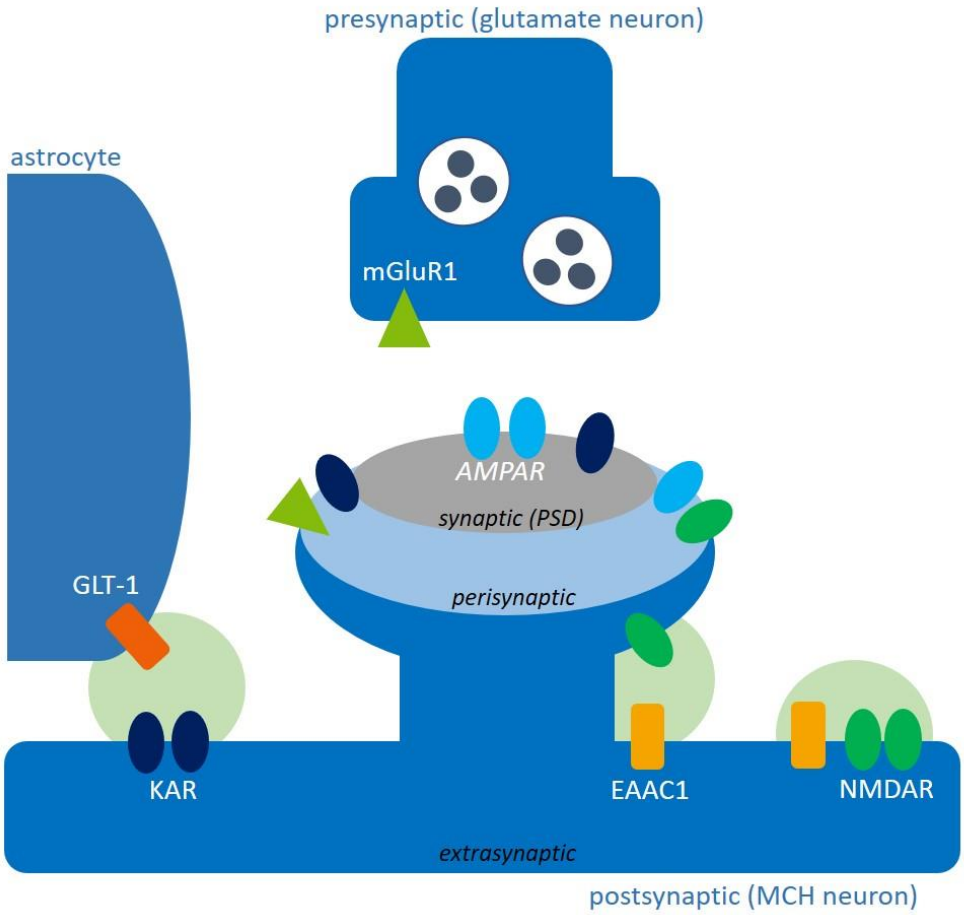

Fig 13. Predicted Subcellular localization of glutamate receptors and transporters in MCH neurons.

Synaptic glutamate: Synaptic receptors associated with postsynaptic density (PSD) mediate the fast EPSCs while perisynaptic receptors activated by spillover glutamate mediate the slow EPSC.

Ambient glutamate: Extrasynaptic receptors mediate tonic current induced by transporter inhibition. GLT-1 tightly regulates extrasynaptic KAR activity and EAAC1 regulates activity at extrasynaptic NMDARs.

Green circles represent predicted regulatory zones of individual glutamate transporter types.

4-12 Future directions

Stepwise currents. A unique pattern emerged during TFB-TBOA induced tonic current that was not present with any other glutamate transporter inhibitors tested. Regardless of concentration, TFB-TBOA resulted in stepwise currents (i.e. rapid shifts in inward current) riding on top of the tonic currents (Fig 9A arrows). These steps ranged in amplitude (approximately 50-250 pA) and occurrence (1-4 steps/cell) but were consistently observed between cells. Further, these steps do not appear to be due to action potential dependent release of glutamate as they persisted in the presence of TTX. While we did not include a thorough analysis of these stepwise currents in the present study, this should be addressed in future research in order to clarify the physiological significance and mechanism underlying this phenomenon. Criteria for defining one individual step will need to be determined, including (but not limited to): amplitude threshold, rise time and decay time.

EAAC1. When compared to iGluRs and mGluRs, glutamate transporters lack the pharmacological tools necessary to define their exact contributions to the regulation of extracellular glutamate levels (Dunlop, 2006). Our preliminary results using an intracellular antibody against EAAC1 were incomplete and inconclusive. Thus, we were only able to determine the EAAC1 contribution indirectly by method of subtraction of TFB-TBOA and DHK induced tonic current. Should an inhibitor for EAAC1 become available, future studies should test it alone and in combination with other glutamate transporter inhibitors to complete a full assessment of transporter contribution at synapses to MCH neurons. The intracellular antibody should be tested more thoroughly at different

concentrations and compared against a control antibody. Alternatively, a transgenic model could be used to determine the role of EAAC1 by knocking out or overexpressing the gene selectively in MCH neurons.

GABAergic signaling. We have characterized excitatory transmission to MCH neurons yet inhibitory GABAergic signaling remains unexplored. Future studies can investigate the effects of GABA transporter inhibitors on inhibitory post synaptic currents and determine which GABA receptors and transporters are important in inhibitory transmission.

4-13 Conclusions/implications

The present study identified several distinct forms of excitatory glutamatergic transmission to MCH neurons of the lateral hypothalamus. We have characterized the distinct magnitude and time courses of glutamate signaling mediated by different glutamate receptors regulated by different transporters. Based on our findings, we have estimated the subcellular location of the receptors and transporters of interest. Thus, this thesis illustrates the complexity of glutamatergic signaling in the nervous system in general and indicates that MCH neurons are an excellent model to investigate this.

In the context of homeostatic mechanisms such as energy balance and sleep wake states, research often focuses on the downstream effects of MCH neuropeptide. The upstream influence of glutamatergic action receives less attention, however this excitatory signaling that regulates cell excitability is crucial to the output of MCH neurons. Glutamate

transporters are an important component of this control, as transporter localization can change under various physiological conditions which influences neurotransmission (Murphy-Royal et al., 2015; Briggs et al. 2018). Thus, this thesis contributes to the fundamental understanding of glutamatergic signaling in the CNS and highlights glutamate transporters as potential modulators of homeostatic mechanisms.

5-0 References

Abrahamsen B, Schneider N, Erichsen MN, Huynh THV, Fahlke C, Bunch L, Jensen AA (2013) Allosteric modulation of an excitatory amino acid transporter: The subtype-selective inhibitor UCPH-101 exerts sustained inhibition of EAAT1 through an intramonomeric site in the trimerization domain. J Neurosci 33:1068–1087.

Arriza JL, Eliasof S, Kavanaugh MP, Amara SG (1997) Excitatory amino acid transporter 5, a retinal glutamate transporter coupled to a chloride conductance. Proc Natl Acad Sci U S A 94:4155–4160.

Barbosa DAN, de Oliveira-Souza R, Santo FM, Faria AC de O, Gorgulho AA, De Salles AAF (2017) The hypothalamus at the crossroads of psychopathology and neurosurgery. Neurosurg Focus 43:1–11.

Bertrand PP, Galligan JJ (1994) Contribution of chloride conductance increase to slow EPSC and tachykinin current in guinea-pig myenteric neurones. J Physiol 481:47–60.

Bittencourt JC, Presse F, Arias C, Peto C, Vaughan J, Nahon J -L, Vale W, Sawchenko PE (1992) The melanin-concentrating hormone system of the rat brain: An immuno- and hybridization histochemical characterization. J Comp Neurol 319:218–245.

Bonnavion P, Mickelsen LE, Fujita A, de Lecea L, Jackson AC (2016) Hubs and spokes of the lateral hypothalamus: cell types, circuits and behaviour. J Physiol 594:6443–6462.

Briggs C, Hirasawa M, Semba K (2018) Sleep deprivation distinctly alters glutamate transporter 1 apposition and excitatory transmission to orexin and MCH neurons. J

Neurosci 38:2179–17.

Brown JA, Woodworth HL, Leinninger GM (2015) To ingest or rest? Specialized roles of lateral hypothalamic area neurons in coordinating energy balance. Front Syst Neurosci 9:1–25.

Castillo PE, Malenka RC, Nicoll RA (1997) Kainate receptors mediate a slow postsynaptic current in hippocampal CA3 neurons. Nature 388:182–186.

Cavelier P, Hamann M, Rossi D, Mobbs P, Attwell D (2005) Tonic excitation and inhibition of neurons: Ambient transmitter sources and computational consequences. Prog Biophys Mol Biol 87:3–16.

Chee MJS, Pissios P, Prasad D, Maratos-Flier E (2014) Expression of melanin-concentrating hormone receptor 2 protects against diet-induced obesity in male mice. Endocrinology 155:81–88.

Chiu DN, Jahr CE (2017) Extracellular Glutamate in the Nucleus Accumbens Is Nanomolar in Both Synaptic and Non-synaptic Compartments. Cell Rep 18:2576–2583.

d'Incamps BL, Krejci E, Ascher P (2012) Mechanisms shaping the slow nicotinic synaptic current at the Motoneuron-Renshaw Cell Synapse. J Neurosci 32:8413–8423.

Danbolt NC (1994) The high affinity uptake system for excitatory amino acids in the brain. Prog Neurobiol 44:377–396.

Danbolt NC (2001) Glutamate uptake. Prog Neurobiol 65:1–105.

Dehnes Y, Chaudhry FA, Ullensvang K, Lehre KP, Storm-Mathisen J, Danbolt NC (1998) The glutamate transporter EAAT4 in rat cerebellar Purkinje cells: A

glutamate-gated chloride channel concentrated near the synapse in parts of the dendritic membrane facing astroglia. J Neurosci 18:3606–3619.

Dunlop J (2006) Glutamate-based therapeutic approaches: Targeting the glutamate transport system. Curr Opin Pharmacol 6:103–107.

Eguchi N, Hishimoto A, Sora I, Mori M (2016) Slow synaptic transmission mediated by TRPV1 channels in CA3 interneurons of the hippocampus. Neurosci Lett 616:170–176.

Fisher JL, Mott DD (2011) Distinct functional roles of subunits within the heteromeric kainate receptor. J Neurosci 31:17113–17122.

Furness DN, Dehnes Y, Akhtar AQ, Rossi DJ, Hamann M, Grutle NJ, Gundersen V, Holmseth S, Lehre KP, Ullensvang K, Wojewodzic M, Zhou Y, Attwell D, Danbolt NC (2008) A quantitative assessment of glutamate uptake into hippocampal synaptic terminals and astrocytes: New insights into a neuronal role for excitatory amino acid transporter 2 (EAAT2). Neuroscience 157:80–94.

Grewer C, Gameiro A, Rauen T (2014) SLC1 Glutamate Transporters The SLC1 transporter family. Pflugers Arch 466(1):3-24.

Hackett JT, Ueda T (2015) Glutamate Release. Neurochem Res 40:2443–2460.

Hahn JD, Swanson LW (2010) Distinct patterns of neuronal inputs and outputs of the juxtaparaventricular and suprafornical regions of the lateral hypothalamic area in the male rat. Brain Res Rev 64:14–103.

Harney SC, Jane DE, Anwyl R (2008) Extrasynaptic NR2D-containing NMDARs are recruited to the synapse during LTP of NMDAR-EPSCs. J Neurosci 28:11685–11694.

Harthoorn LF, Sañé A, Nethe M, Van Heerikhuize JJ (2005) Multi-transcriptional profiling of melanin-concentrating hormone and orexin-containing neurons. Cell Mol Neurobiol 25:1209–1223.

Haugeto Ø, Ullensvang K, Levy LM, Chaudhry FA, Honoré T, Nielsen M, Lehre KP, Danbolt NC (1996) Brain glutamate transporter proteins form homomultimers. J Biol Chem 271:27715–27722.

Herman MA, Jahr CE (2007) Extracellular glutamate concentration in hippocampal slice. J Neurosci 27:9736–9741.

Hirono M, Konishi S, Yoshioka T (1998) Phospholipase C-independent group I metabotropic glutamate receptor-mediated inward current in mouse Purkinje cells. Biochem Biophys Res Commun 251:753–758.

Hollmann M (1994) Cloned Glutamate Receptors. Annu Rev Neurosci 17:31–108.

Holmseth S, Dehnes Y, Huang YH, Follin-Arbelet V V., Grutle NJ, Mylonakou MN, Plachez C, Zhou Y, Furness DN, Bergles DE, Lehre KP, Danbolt NC (2012) The density of EAAC1 (EAAT3) glutamate transporters expressed by neurons in the mammalian CNS. J Neurosci 32:6000–6013.

Huang H, van den Pol AN (2007) Rapid Direct Excitation and Long-Lasting Enhancement of NMDA Response by Group I Metabotropic Glutamate Receptor Activation of Hypothalamic Melanin-Concentrating Hormone Neurons. J Neurosci 27:11560–11572.

Huang YH, Sinha SR, Tanaka K, Rothstein JD, Bergles DE (2004) Astrocyte glutamate transporters regulate metabotropic glutamate receptor-mediated excitation of hippocampal interneurons. J Neurosci 24:4551–4559.

Jonas P (2000) The time course of signaling at central glutamatergic synapses. News Physiol Sci 15:83–89.

Jourdain P, Bergersen LH, Bhaukaurally K, Bezzi P, Santello M, Domercq M, Matute C, Tonello F, Gundersen V, Volterra A (2007) Glutamate exocytosis from astrocytes controls synaptic strength. Nat Neurosci 10:331–339.

Kawauchi H, Kawazoe I, Tsubokawa M, Kishida M, Baker BI (1983) Characterization of melanin-concentrating hormone in chum salmon pituitaries. Nature 305:321–323.

Kurosinski P, Biol D, Götz J (2002) Glial cells under physiologic and pathologic conditions. Arch Neurol 59:1524–1528.

Lagos P, Torterolo P, Jantos H, Chase MH, Monti JM (2009) Effects on sleep of melanin-concentrating hormone (MCH) microinjections into the dorsal raphe nucleus. Brain Res 1265:103–110.

Le Meur K, Galante M, Angulo MC, Audinat E (2007) Tonic activation of NMDA receptors by ambient glutamate of non-synaptic origin in the rat hippocampus. J Physiol 580:373–383.

Lehre KP, Danbolt NC (1998) The number of glutamate transport subtype molecules at glutamatergic synapses: Chemical and stereological quantification in young adult rat brain. J Neurosci 18:8751–8757.

Lerma J (2003) Roles and rules of kainate receptors in synaptic transmission. Nat Rev Neurosci 4:481–495.

Ludwig DS, Tritos NA, Mastaitis JW, Kulkarni R, Kokkotou E, Elmquist J, Lowell B, Flier JS, Maratos-Flier E (2001) Melanin-concentrating hormone overexpression in transgenic mice leads to obesity and insulin resistance. J Clin Invest 107:379–386.

Marx MC, Billups D, Billups B (2015) Maintaining the presynaptic glutamate supply for excitatory neurotransmission. J Neurosci Res 93:1031–1044.

Meister B (2007) Neurotransmitters in key neurons of the hypothalamus that regulate feeding behavior and body weight. Physiol Behav 92:263–271.

Murphy-Royal C, Dupuis JP, Varela JA, Panatier A, Pinson B, Baufreton J, Groc L, Oliet SHR (2015) Surface diffusion of astrocytic glutamate transporters shapes synaptic transmission. Nat Neurosci 18:219–226.

Niswender CM, Conn PJ (2010) Metabotropic Glutamate Receptors: Physiology, Pharmacology, and Disease. Annu Rev Pharmacol Toxicol 50:295–322.

Oleg J (1966) Simple allosteric model for membrane pumps. Nature 211:969–970.

Ottersen OP, Zhang N, Walberg F (1992) Metabolic compartmentation of glutamate and glutamine: Morphological evidence obtained by quantitative immunocytochemistry in rat cerebellum. Neuroscience 46:519–534.

Pál B (2015) Astrocytic actions on extrasynaptic neuronal currents. Front Cell Neurosci 9:1–11.

Papouin T, Oliet SHR (2014) Organization, Control and function of extrasynaptic NMDA receptors. Philos Trans R Soc B Biol Sci 369:18–21.

Povysheva N V., Johnson JW (2012) Tonic NMDA receptor-mediated current in prefrontal cortical pyramidal cells and fast-spiking interneurons. J Neurophysiol 107:2232–2243.

Reiner A, Levitz J (2018) Glutamatergic Signaling in the Central Nervous System: Ionotropic and Metabotropic Receptors in Concert. Neuron 98:1080–1098.

Rusakov DA (2009) UKPMC Funders Group synapses. 12:317–326.

Scheefhals N, MacGillavry HD (2018) Functional organization of postsynaptic glutamate receptors. Mol Cell Neurosci 91:82–94.

Schmitt A, Asan E, Püschel B, Kugler P (1997) Cellular and regional distribution of the glutamate transporter GLAST in the CNS of rats: Nonradioactive in situ hybridization and comparative immunocytochemistry. J Neurosci 17:1–10.

Schousboe A (1981) Transport and metabolism of glutamate and gaba in neurons and glial cells.

Scimemi A, Tian H, Diamond JS (2009) Neuronal transporters regulate glutamate clearance, NMDA receptor activation, and synaptic plasticity in the hippocampus. J Neurosci 29:14581–14595.

Sheng N, Yang J, Silm K, Edwards RH, Nicoll RA (2017) A slow excitatory postsynaptic current mediated by a novel metabotropic glutamate receptor in CA1 pyramidal neurons. Neuropharmacology 115:4–9.

Shimada M, Tritos NA, Lowell BB, Flier JS, Maratos-Flier E (1998) Mice lacking melanin-concentrating hormone are hypophagic and lean. Nature 396:670–679.

Steinert JR, Postlethwaite M, Jordan MD, Chernova T, Robinson SW, Forsythe ID (2010) NMDAR-mediated EPSCs are maintained and accelerate in time course during maturation of mouse and rat auditory brainstem in vitro. J Physiol 588:447–463.

Stincic TL, Frerking ME (2015) Different AMPA receptor subtypes mediate the distinct kinetic components of a biphasic EPSC in hippocampal interneurons. Front Synaptic Neurosci 7:1–11.

Sun YG, Pita-Almenar JD, Wu CS, Renger JJ, Uebele VN, Lu HC, Beierlein M (2013) Biphasic cholinergic synaptic transmission controls action potential activity in

thalamic reticular nucleus neurons. J Neurosci 33:2048–2059.

Tasker JG, Oliet SHR, Bains JS, Brown CH, Stern JE (2012) Glial Regulation of Neuronal Function: From Synapse to Systems Physiology. J Neuroendocrinol 24:566–576.

Traynelis SF et al (2010) Glutamate receptor review. Pharmacol Rev 14:37–40.

Trotti D, Danbolt NC, Volterra A (1998) Glutamate transporters are oxidant-vulnerable: A molecular link between oxidative and excitotoxic neurodegeneration? Trends Pharmacol Sci 19:328–334.

Tsukada S, Iino M, Takayasu Y, Shimamoto K, Ozawa S (2005) Effects of a novel glutamate transporter blocker, (2S, 3S)-3-{3-[4-(trifluoromethyl)benzoylamino]benzyloxy}aspartate (TFB-TBOA), on activities of hippocampal neurons. Neuropharmacology 48:479–491.

Vandenberg RJ, Ryan RM (2013) Mechanisms of glutamate transport. Physiol Rev 93:1621–1657.

Verret L, Goutagny R, Fort P, Cagnon L, Salvert D, Léger L, Boissard R, Salin P, Peyron C, Luppi P (2003) Central Regulation of Paradoxical Sleep. BMC Neurosci 10:1–10.

Vyleta NP, Smith SM (2011) Spontaneous glutamate release is independent of calcium influx and tonically activated by the calcium-sensing receptor. J Neurosci 31:4593–4606.

Weilinger NL, Lohman AW, Rakai BD, Ma EMM, Bialecki J, Maslieieva V, Rilea T, Bandet M V., Ikuta NT, Scott L, Colicos MA, Teskey GC, Winship IR, Thompson RJ (2016) Metabotropic NMDA receptor signaling couples Src family kinases to pannexin-1 during excitotoxicity. Nat Neurosci 19:432–442.

Wondolowski J, Frerking M (2009) Subunit-dependent postsynaptic expression of kainate receptors on hippocampal interneurons in area CA1. J Neurosci 29:563–574.

Zampini V, Liu JK, Diana MA, Maldonado PP, Brunel N, Dieudonné S (2016) Mechanisms and functional roles of glutamatergic synapse diversity in a cerebellar circuit. Elife 5:1–25.

Zerangue N, Kavanaugh MP (1996) Flux coupling in a neuronal glutamate transporter. Nature 383:634–637.

Zhou Y, Danbolt NC (2014) Glutamate as a neurotransmitter in the healthy brain. J Neural Transm 121:799–817.